

Electronic Supplementary Information for

Ambient Synthesis of Metal-Covalent Organic Frameworks with Fe-Iminopyridine Linkage

Tiantian Feng,^{a,b} Bing Sun,^{a,*} Qing Hao,^b Jing Li,^c Ying Xu,^b Hong Shang,^a Dong Wang^{b,*}

a School of Science, China University of Geosciences, Beijing 100083, P. R. China

b Key Laboratory of Molecular Nanostructure and Nanotechnology, Institute of Chemistry, Chinese Academy of Sciences and Beijing National Laboratory for Molecular Sciences, Beijing 100190, P. R. China

c Key Laboratory of Bio-inspired Smart Interfacial Science and Technology of Ministry of Education, School of Chemistry, Beihang University, Beijing 100191, P. R. China

* Corresponding authors:

Bing Sun: sunbing@cugb.edu.cn

Dong Wang: wangd@iccas.ac.cn

Contents

S1. Experimental details	S1
S1.1 Materials	S1
S1.2 Instrument and characterization.....	S2
S1.3 Crystal Structure modeling and refinements	S5
S1.4 Synthesis of Fe-COF _{TTA-BPA} and P(TTA-BPA).....	S6
S1.5 Synthesis of Fe-COF _{TAPB-BPA}	S6
S1.6 Synthesis of Fe-COF _{TTA-PDA}	S7
S1.7 Synthesis of Fe-COF _{TAPB-PDA}	S7
S2. Synthesis and characterization of model compounds	S8
S2.1 Synthesis and characterization of model compound 1	S8
S2.2 Synthesis and characterization of model compound [Fe- 1](OTf) ₈	S9
S2.3 Synthesis and characterization of model compound [Fe- 2](OTf) ₈	S10
S3. Synthesis and characterization of BPA-based Fe-COFs.....	S11
S3.1 Synthetic optimization.....	S11
S3.2 Crystal structure and stacking models	S17
S3.3 Morphologies.....	S20
S3.4. Isotherms and pore size distribution	S22
S3.5 Solid-state ¹³ C NMR and FTIR spectra.....	S24
S3.6 XPS spectra.....	S29
S3.7 EXAFS fitting.....	S35
S3.8 Paramagnetic properties.....	S36
S4. Control experiments.....	S37
S5. Synthesis and characterization of PDA-based Fe-COFs.....	S40
S5.1 Crystalline structure and stacking models	S40
S5.2 TEM and HAADF-STEM images	S44
S5.3 Isotherms and pore size distribution of Fe-COFs	S46
S5.4 Solid-state ¹³ C NMR, FTIR, and XPS spectra.....	S49
S6. Atomic parameters of refined Fe-COF models and calculated parameters.	S52
References.....	S68

S1. Experimental details

S1.1 Materials

4,4',4''-(1,3,5-triazine-2,4,6-triyl)trianiline (TTA), 1,3,5-tris(4-aminophenyl)benzene (TAPB), 4,4'-biphenyldicarboxaldehyde (BPDA), and 2,2'-bipyridine-5,5'-dicarboxaldehyde (iso-BPA) were purchased from TCI Chemicals. Mesitylene, 1,4-dioxine, *o*-dichlorobenzene (*o*-DCB) and acetonitrile (MeCN) were supplied by Acros Organics. Iron(II) trifluoromethanesulfonate ($\text{Fe}(\text{OTf})_2$), copper(II) trifluoromethanesulfonate ($\text{Cu}(\text{OTf})_2$), (trifluoromethylsulfonyloxy) copper(I) ($\text{Cu}_2(\text{OTf})_2$), zinc trifluoromethanesulfonate ($\text{Zn}(\text{OTf})_2$), zinc perchlorate ($\text{Zn}(\text{ClO}_4)_2$), iron(II) tetrafluoroborate hexahydrate ($\text{Fe}(\text{BF}_4)_2 \cdot 6\text{H}_2\text{O}$), iron(II) acetate ($\text{Fe}(\text{CH}_3\text{COO})_2$), zinc tetrafluoroborate hydrate ($\text{Zn}(\text{BF}_4)_2 \cdot \text{H}_2\text{O}$), calcium trifluoromethanesulfonate ($\text{Ca}(\text{OTf})_2$), scandium(III) trifluoromethanesulfonate ($\text{Sc}(\text{OTf})_3$), yttrium(III) trifluoromethanesulfonate ($\text{Y}(\text{OTf})_3$), nickel(II) trifluoromethanesulfonate ($\text{Ni}(\text{OTf})_2$) and acetic acid were supplied by J&K Chemical. All other chemicals are commercially available and used directly without further purification.

3,3'-Bipyridine-6,6'-dicarboxaldehyde (BPA) was synthesized from 5-bromo-2-pyridinecarboxaldehyde (TCI Chemicals) according to the previous method.^[S1] The chemical structure of BPA was confirmed by NMR spectroscopy. ^1H NMR (400 MHz, 298 K, CD_3CN): δ = 10.12 ppm (*s*, 2H), 9.15 ppm (*s*, 2H), 8.31 ppm (*d*, 2H), 8.07 ppm (*d*, 2H). ^{13}C NMR (400 MHz, 298 K, CDCl_3): δ = 192.3, 151.3, 145.2, 135.7, 134.6, 121.3 ppm.

Pyrazine-2,5-dicarbaldehyde (PDA) was synthesized from 2,5-dimethyl pyrazine

according to the previous method.^[S2] The chemicals structure of BPA was confirmed by NMR spectroscopy. ¹H NMR (400 MHz, 298 K, CDCl₃): δ = 10.21 ppm (s, 2H), 9.33 ppm (s, 2H). ¹³C NMR (400 MHz, 298 K, CDCl₃): δ = 192.6, 149.8, 144.2 ppm.

S1.2 Instrument and characterization

Powder X-ray diffraction (PXRD). PXRD patterns were recorded on a PANalytical Empyrean Diffractometer operated at 40 kV and 40 mA with Cu Kα radiation ($\lambda = 1.5416 \text{ \AA}$) ranging from 1.5 to 40° with a speed of 2 °/min at ambient temperature.

FT-IR spectra. FT-IR spectra were recorded in transmission mode by loading samples with KBr planet on a Bruker RFS100/S instrument in the range of 400 to 4000 cm⁻¹ with an interval of 4 cm⁻¹.

NMR spectra. NMR spectra (¹H and ¹³C) and solid-state ¹³C NMR spectra were recorded on a Bruker AVANCE III 600 M NMR spectrometer at ambient temperature (298 K). Deuterated chloroform (CDCl₃) or acetonitrile (CD₃CN) was used as a solvent for ¹H and ¹³C NMR spectroscopy measurement of synthesized molecule building blocks and mode compounds.

Microstructural observation. Morphology observation was performed using JEM-2100F transmission electron microscopy (TEM) at an accelerating voltage of 200 kV and JEOL SU8020 field-emission scanning electron microscopy (SEM). TEM samples were prepared by dropping the sample from anhydrous ethanol on copper grids supporting a thin, electron transparent carbon film. HAADF-STEM analyses were performed on an aberration-corrected JEOL ARM-200F system equipped with a cold

field emission gun and an ASCOR probe corrector at 60 kV. The imaging dose rate for single frame imaging is estimated as 8×10^5 e/nm²·s with a total dose of 1.6×10^7 e/nm².

Porous structure analysis. Nitrogen adsorption and desorption isotherms were measured using Micromeritics ASAP-2020 Surface Area and Porosity Analyzer. The samples loaded in sample tubes were heated to 90 °C under a vacuum of 0.5 mtorr for 24 h, and the measurements were conducted at liquid nitrogen temperature (77 K) using ultrahigh-purity grade nitrogen (99.999%).

MALDI-TOF-MS. MALDI-TOF-MS analysis was performed on a Bruker Autoflex III time-of-flight (TOF) mass spectrometer (MS), equipped with a smartbeamTM-II laser (354 nm wavelength, Bruker), in the reflection (or in the linear) mode. Around 1000 spectra were summed at a scan rate of 2 kHz in the mass (*m/z*) range of 300 to 1500.

X-ray photoelectron spectroscopy (XPS). XPS spectra were performed on the Thermo Scientific ESCALab 250Xi using 200 W monochromated Al K α radiation. The 500 μ m X-ray spots were used for XPS analysis. The base pressure in the analysis chamber was about 3×10^{-10} mbar. Typically, the hydrocarbon C1s line at 284.8 eV from adventitious carbon is used for energy referencing. The background of all spectra was subtracted using a Shirley-type background to remove most of the extrinsic loss structure.

X-ray absorption fine structure (XAFS). XAFS measurements were performed in the 1W1B line station of the Beijing Synchrotron Radiation Faculty. X-ray beam parameters for XAFS analysis were $>5 \times 10^{11}$ photons/s@9 keV, photon energy of 2.5

GeV, and beam current of 200 mA. The beam spot was $0.9(H) \times 0.3(V)$ mm². Iron foil and FeFc were used as the reference standards. All experiments were performed at ambient conditions. The spectra were plotted using Athene and Artemis softwares based on the simulated Fe-COF crystalline structure files.

The XAFS data were processed using the ATHENA module implemented in the IFEFFIT software packages via the standard procedures. The k^3 -weighted EXAFS spectra were obtained by subtracting the post-edge background from the overall absorption and then normalizing with respect to the edge-jump step. k^3 -Weighted $\chi(k)$ data of Fe K-edge were Fourier transformed to real (R) space using a hanning window ($dk = 1.0 \text{ \AA}^{-1}$) to separate the EXAFS contributions from different coordination shells. The ARTEMIS module of IFEFFIT software packages was used to obtain the quantitative structural parameters around central atoms, least-squares curve parameter fitting. The following EXAFS equation was used:

$$\chi(k) = \sum_j \frac{N_j S_0^2 F_j(k)}{k R_j^2} \exp[-2k^2 \sigma_j^2] \exp\left[\frac{-2R_j}{\lambda(k)}\right] \sin[2kR_j + \phi_j(k)]$$

where S_0^2 is the amplitude reduction factor, $F_j(k)$ is the effective curved-wave backscattering amplitude, N_j is the number of neighbors in the j^{th} atomic shell, R_j is the distance between the X-ray absorbing central atom and the atoms in the j^{th} atomic shell (backscatter), λ is the mean free path in Å, $\phi_j(k)$ is the phase shift (including the phase shift for each shell and the total central atom phase shift), σ_j is the Debye-Waller parameter of the j^{th} atomic shell (variation of distances around the average R_j). The functions $F_j(k)$, λ and $\phi_j(k)$ were calculated with the *ab initio* code FEFF8.2

Magnetic susceptibility measurements. The temperature-dependence magnetic

susceptibility measurements of the sample constituted of monocrystals (~10 mg) were carried out on a Quantum Design Physical Property Measurement System (PPMS®) at field strengths of 5 kOe in the heating mode within a temperature range from 2 to 300 K. The M-H curves were measured under the field strengths of ± 50 kOe. Gelatine capsules were used as sample containers for measurements. The data were corrected for the magnetization of the sample holder, and diamagnetic corrections were estimated using Pascal's constants [S³]. Molar susceptibility (χ_M) per molar iron was used to illustrate the paramagnetic performance of Fe-COFs and model compounds. The Curie-Weiss law was accounted for χ_M vs. T plot of the experimental magnetization curve. Effective magnetic moment (μ_{eff}) was estimated by the following function:

$$\mu_{\text{eff}} = \sqrt{\frac{3k_B T \chi_M}{N_A}} = 2.828\sqrt{\chi_M T} \mu_B$$

where, N_A , k_B , T , χ_M represent Avogadro constant, represents Boltzmann constant, temperature, and molar susceptibility, respectively. μ_B is Bohr magnetic moments.

The spin state of Fe(II) in Fe-COFs was also estimated by calculating the total spin angular momentum (S) based on:

$$\mu_{\text{eff}} = \mu_B g \sqrt{\sum S(S+1)}$$

where g is the Lander factor (which is generally as 2.03 for Fe coordinating compound).

S1.3 Crystal Structure modeling and refinements

The crystal models for Fe-COFs were modeled by using Materials Studio 5.0 software package (Accelrys Software Inc. (2009, now BIOVIA). Materials Studio 5.0: Modeling Simulation for Chemical and Material, San Diego, CA.). The lattice

parameters and atomic positions were optimized under the universal force field and were further refined through the Pawley PXRD refinement conducted with the Reflex module until the R_{wp} value converged and a good agreement was obtained between the refined profiles and the experimental ones. The parameters including peak broadening, peak asymmetry, and zero shift error were considered in the applied Pseudo-Voigt profile function for whole profile refinement.

S1.4 Synthesis of Fe-COF_{TTA-BPA} and P(TTA-BPA)

Fe-COF_{TTA-BPA} was rapidly synthesized from the polycondensation of TTA and BPA in the presence of Fe(OTf)₂ and acetic acid at room temperature. Typically, TTA (28.35 mg, 0.08 mmol), BPA (25.46 mg, 0.12 mmol), Fe(OTf)₂ (28.32 mg, 0.08 mmol) and mixed solvent of 1,4-dioxane and mesitylene (1 mL, v/v = 1:1) were charged into a cylinder glass-tube and sonically treated to obtain a celadon homogeneous suspension. Then, acetic acid aqueous (6 mol L⁻¹) with various volumes was added. The mixture was kept at room temperature or lower temperature for a few minutes to get the tan precipitates. The powders were collected by centrifugation, rinsed by tetrahydrofuran (THF), activated in Soxhlet extraction system with THF as solvent over 24 hours, and finally drought at 80 °C under vacuum conditions. Amorphous porous polymer (P(TTA-BPA)) was synthesized by using a similar method except for the absence of Fe(OTf)₂.

S1.5 Synthesis of Fe-COF_{TAPB-BPA}

Fe-COF_{TAPB-BPA} was synthesized from the polycondensation of TAPB and BPA in the presence of Fe(OTf)₂ and acetic acid at room temperature. Typically, TAPB (28.12 mg, 0.08 mmol), BPA (25.46 mg, 0.12 mmol), Fe(OTf)₂ (28.32 mg, 0.08 mmol) and a

mixed solvent of 1,4-dioxane and mesitylene (1 mL, v/v = 1:1) and acetic acid aqueous (6 mol L⁻¹, 400 µL) were charged into a cylinder glass-tube for the synthesis of Fe-COF_{TAPB-BPA} at room temperature or lower temperature for few minutes. The brown powders were obtained following the same treatment as described above.

S1.6 Synthesis of Fe-COF_{TTA-PDA}

Fe-COF_{TTA-PDA} was synthesized from the polycondensation of TTA and PDA in the presence of Fe(OTf)₂ and acetic acid at room temperature. Typically, TTA (28.35 mg, 0.08 mmol), PDA (16.33 mg, 0.12 mmol), Fe(OTf)₂ (27.96 mg, 0.08 mmol), *o*-DCB (1 mL) and acetic acid aqueous (6 mol L⁻¹, 400 µL) were charged into a cylinder glass-tube for the synthesis of Fe-COF_{TTA/PDA} at room temperature for few minutes. The brown powders were obtained following the same treatment as described above.

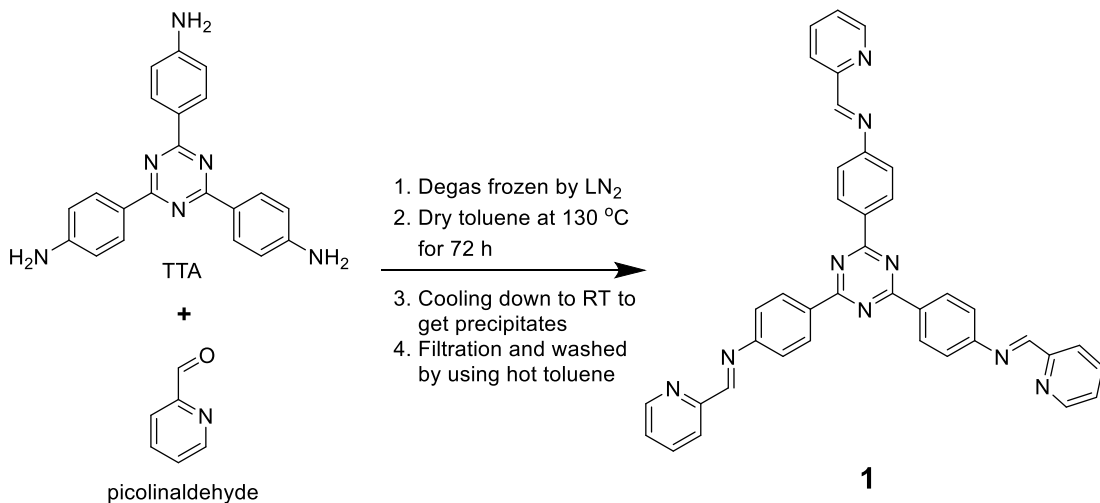
S1.7 Synthesis of Fe-COF_{TAPB-PDA}

Fe-COF_{TAPB-PDA} was synthesized from the polycondensation of TAPB and PDA in the presence of Fe(OTf)₂ and acetic acid at room temperature. Typically, TAPB (28.11 mg, 0.08 mmol), PDA (16.33 mg, 0.12 mmol), Fe(OTf)₂ (27.96 mg, 0.08 mmol), *o*-DCB (1 mL), and acetic acid aqueous (6 mol L⁻¹, 400 µL) were charged into a cylinder glass-tube for the synthesis of Fe-COF_{TTA-PDA} at room temperature for few minutes. The brown powders were obtained following the same treatment as described above.

S2. Synthesis and characterization of model compounds

S2.1 Synthesis and characterization of model compound 1

Scheme S1. Synthesis of model compound **1** from TTA and picinaldehyde.



Model compound **1** was synthesized from the reaction of TTA and picinaldehyde.

TTA (28.4 mg, 0.08 mmol), picinaldehyde (135.85 mg, 12 equiv.), and a Teflon-covered magnetic stirring bar were charged in a 20 mL microwave vial, which was sealed and degassed via three freeze-pump-thaw cycles under nitrogen atmosphere. Purified dry toluene (5 mL) was added to the above vial through a syringe. The mixture was heated to 130 °C for 72 h with stirring. The off-white powders precipitated from the mixture as cooling down to room temperature, and further collected by filtration and washed by using hot toluene (*Notes: The model compound can easily dissolve in chloroform, not dissolve in cold toluene. The precursor TTA cannot dissolve in chloroform.*). ^1H NMR (600 MHz, Chloroform-*d*) δ 8.94 – 8.88 (m, 6H), 8.80 (d, J = 4.7 Hz, 3H), 8.73 (s, 3H), 8.30 (d, J = 7.9 Hz, 3H), 7.91 (t, J = 7.7 Hz, 3H), 7.53 – 7.43

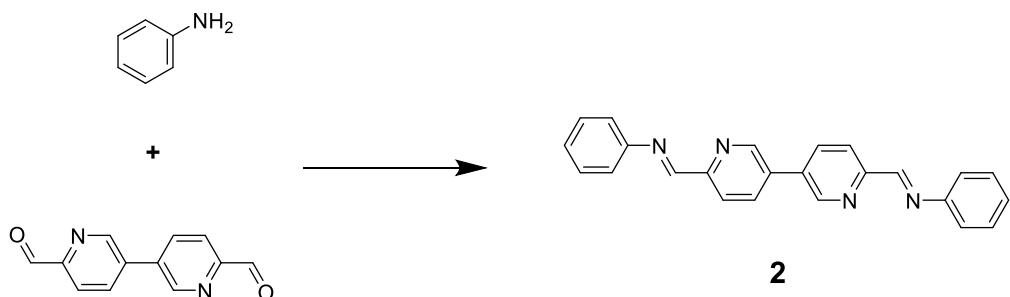
(m, 9H). ^{13}C NMR (151 MHz, Chloroform-*d*) δ 171.02, 161.76, 154.83, 154.31, 149.88 (d, J = 2.6 Hz), 136.81, 134.47, 130.27, 125.40, 122.21, 121.31. MALDI-TOF-MS *m/z*: 622.332 [M+H]⁺, 623.326, 624.342, 620.318, 621.321 (calculated molecular weight 621.71 for C₃₉H₂₇N₉).

S2.2 Synthesis and characterization of model compound [Fe-1](OTf)₈

The [Fe-1](OTf)₈ was synthesized from TTA and picolinaldehyde in the presence of Fe(OTf)₂. TTA (35.44 mg, 0.10 mmol), picolinaldehyde (42.80 mg, 0.40 mmol), Fe(OTf)₂ (35.40 mg, 0.10 mmol) and a Teflon-covered magnetic stirring bar were charged in a 20 mL microwave vial, which was sealed and degassed via three freeze-pump-thaw cycles under nitrogen atmosphere. Purified dry MeCN (3 mL) was added in the above vial through a syringe. The mixture was heated to 100 °C for 24 h with stirring. After cooling down to room temperature, [Fe-1](OTf)₈ was precipitated as a purple powder by dropping the mixture to anhydrous diethyl ether, further collected by centrifugation, washed by diethyl ether twice times, and dried under vacuum. ^1H NMR (600 MHz, Acetonitrile-*d*₃) δ 9.03 (s, 3H), 8.72 (d, J = 8.2 Hz, 3H), 8.65 (d, J = 7.6 Hz, 3H), 8.51 (ddd, J = 26.4, 17.1, 8.0 Hz, 9H), 7.85 (t, J = 6.7 Hz, 3H), 7.48 (d, J = 5.5 Hz, 3H), 6.81 (d, J = 8.8 Hz, 3H), 6.04 (d, J = 8.2 Hz, 3H), 4.96 (s, 3H), 4.72 (d, J = 8.4 Hz, 3H). ^{13}C NMR (151 MHz, Acetonitrile-*d*₃) δ 175.96, 172.99, 170.12, 159.04, 157.13, 156.50, 140.87, 137.43, 131.89, 124.96, 123.05, 122.53. MALDI-TOF-MS *m/z*: 533.411 [[Fe-1]+2OTf]⁶⁺, 622.455 [[Fe-1]+3OTf]⁵⁺, 841.581 [[Fe-1]+4OTf]⁴⁺, calculated molecular weight 3902.71 for C₁₆₄H₁₀₈F₂₄Fe₄N₃₆O₂₄S₈.

S2.3 Synthesis and characterization of model compound [Fe-2](OTf)₈

Scheme S2. Synthesis of model compound **2**.



The [Fe-2](OTf)₈ was synthesized by the reaction of BPA and aniline in the presence of Fe(OTf)₂ modified from previous work.^[S4] Typically, BPA (50.85 mg, 0.24 mmol), aniline (45.30 mg, 0.48 mmol), Fe(OTf)₂ (56.63 mg, 0.16 mmol) and a Teflon-covered magnetic stirring bar were added in a 20 mL microwave vial. The vial was sealed and subjected to freeze-pump-thaw cycles to remove oxygen. Purified dry MeCN (6 mL) was added to the above vial through a syringe. The mixture was heated to 70 °C for 48 h with stirring. Then [Fe-2](OTf)₈ was precipitated as a purple powder by the addition of diisopropyl ether, further collected by centrifugation, washed by diethyl ether twice times, and dried under vacuum. ¹H NMR (600 MHz, Acetonitrile-*d*₃) δ 9.19 (s, 2H), 8.67 (d, *J* = 8.3 Hz, 2H), 8.32 (d, *J* = 8.0 Hz, 2H), 7.43 (t, *J* = 7.7 Hz, 2H), 7.24 (t, *J* = 7.6 Hz, 4H), 7.17 (s, 2H), 5.50 (d, *J* = 7.8 Hz, 4H). ¹³C NMR (151 MHz, Acetonitrile-*d*₃) δ 175.36, 158.61, 155.51, 151.43, 141.44, 138.46, 131.25, 130.41, 129.87, 122.25. MALDI-TOF-MS *m/z*: 433.395 [[Fe-2]+2OTf]⁶⁺, 567.247 [[Fe-2]+3OTf]⁵⁺, 723.538 [[Fe-2]+4OTf]⁴⁺, 992.701 [[Fe-2]+5OTf]³⁺, calculated molecular weight 3590.50 for C₁₅₂H₁₀₈F₂₄Fe₄N₂₄O₂₄S₈.

S3. Synthesis and characterization of BPA-based Fe-COFs.

S3.1 Synthetic optimization

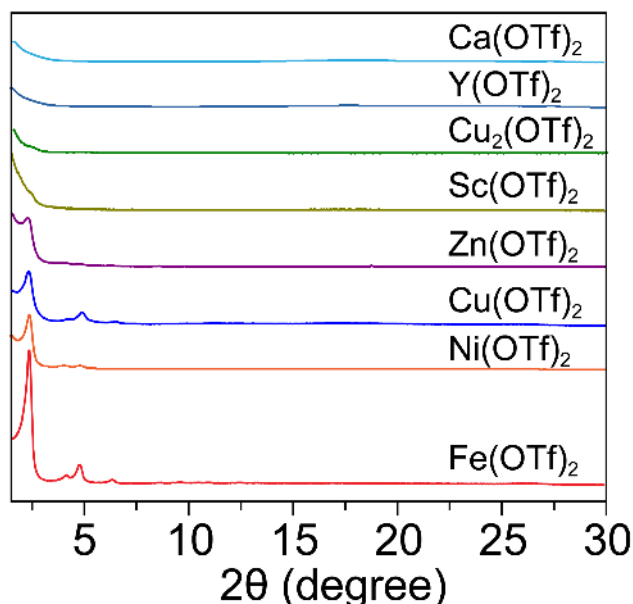


Fig. S1 Effect of $\text{M}(\text{OTf})_2$ on the PXRD patterns with 6 M HOAc in the mixed solvents of dioxane/mesitylene (v:v = 1:1) at room temperature for 20 min.

Fe-COFs show the best crystallinity compared to the other crystalline MCOFs constructed with Ni^{2+} , Cu^{2+} , or Zn^{2+} in the presence of trifluoromethanesulfonic (OTf^-) anions and HOAc. No prominent diffraction peaks are detected in the case of $\text{Sc}(\text{OTf})_2$, $\text{Cu}_2(\text{OTf})_2$, $\text{Ca}(\text{OTf})_2$, and $\text{Y}(\text{OTf})_2$, indicating the different growing dynamic for Fe-COFs compared to the previous imine COFs catalyzed by $\text{Sc}(\text{OTf})_2$.

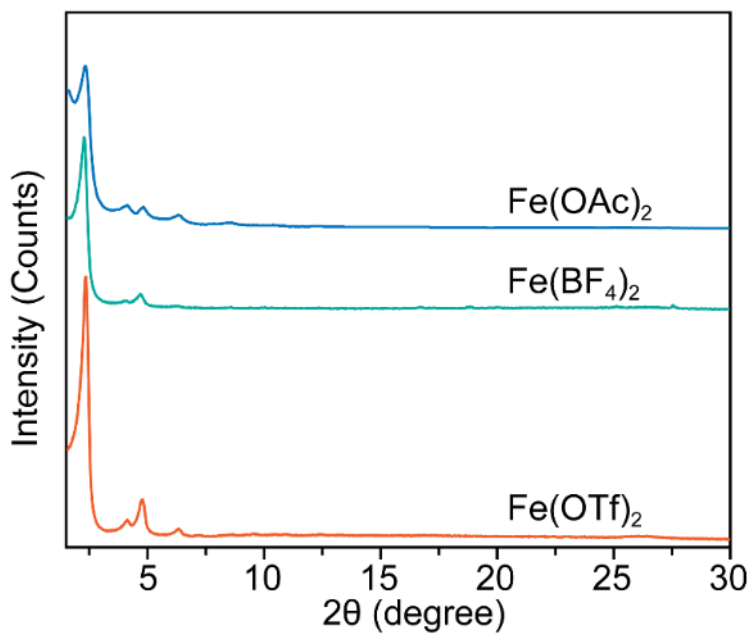


Fig. S2 PXRD patterns of $\text{Fe-COF}_{\text{TTA-BPA}}$ synthesized in the mixed solvents of dioxane/mesitylene (v:v =1:1) with $\text{Fe}(\text{OTf})_2$, $\text{Fe}(\text{BF}_4)_2$, and $\text{Fe}(\text{OAc})_2$ for 20 min.

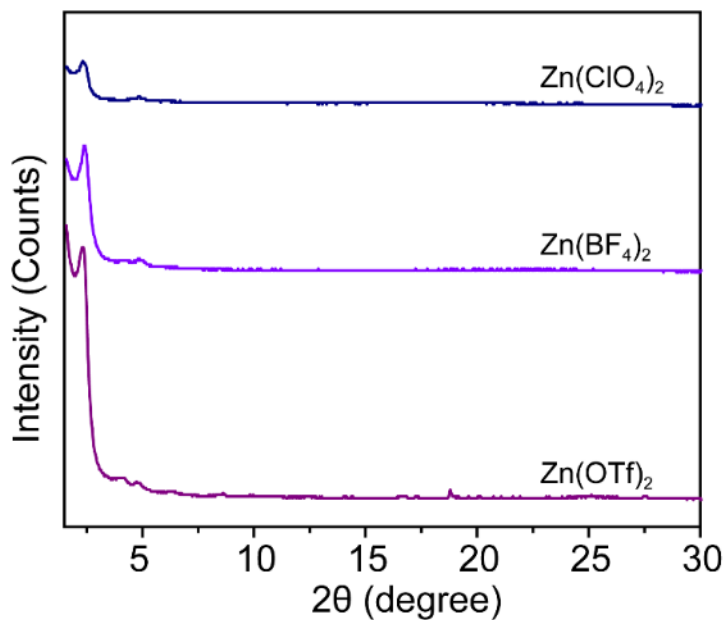


Fig. S3 PXRD patterns of $\text{Zn-COF}_{\text{TTA-BPA}}$ synthesized in the mixed solvents of dioxane/mesitylene (v:v =1:1) with $\text{Zn}(\text{OTf})_2$, $\text{Zn}(\text{BF}_4)_2$, and $\text{Zn}(\text{ClO}_4)_2$, respectively. The OTf^- represents the better anion for crystalline Fe-COF preparation than BF_4^- , OAc^- or ClO_4^- .

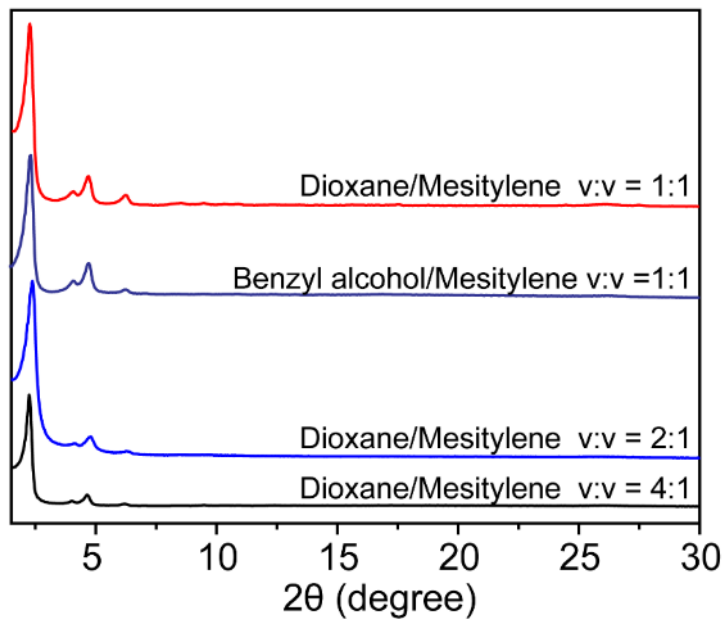


Fig. S4 PXRD patterns of Fe-COF_{TTA-BPA} synthesized at room temperature in the different mixed solvents with the catalysis of both HOAc and Fe(OTf)₂.

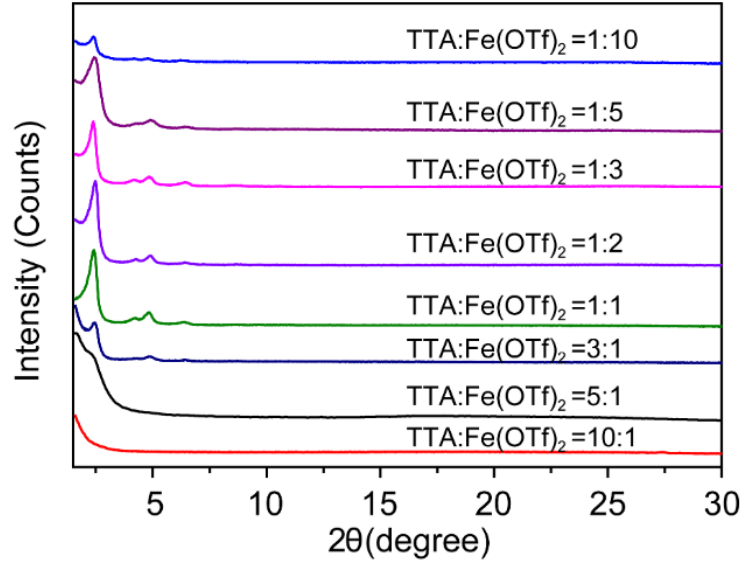


Fig. S5 PXRD patterns of Fe-COF_{TTA-BPA} synthesized at ambient conditions in dioxane/mesitylene (v/v = 1:1) with a different molar ratio of TTA to Fe(OTf)₂ in the presence of 6 M HOAc.

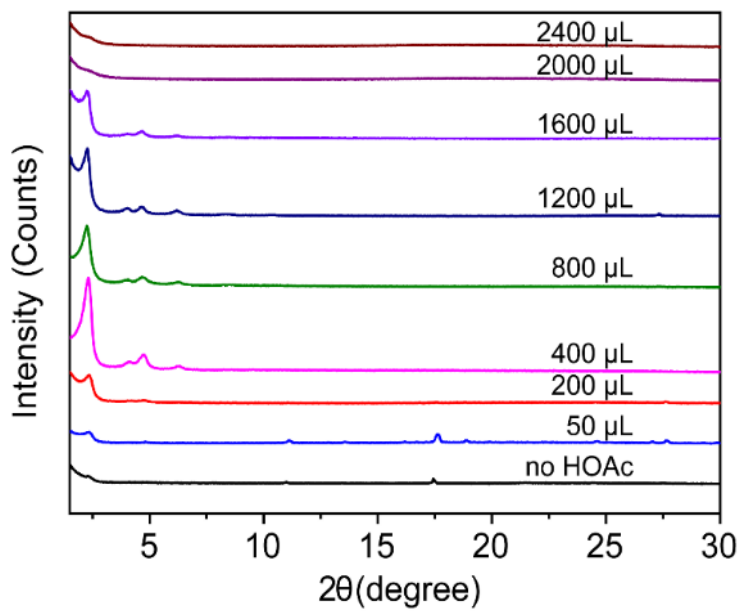


Fig. S6 PXRD patterns of Fe-COF_{TTA-BPA} synthesized at ambient conditions in dioxane/mesitylene (v/v =1:1) with different volumes of 6 M HOAc in the presence of Fe(OTf)₂.

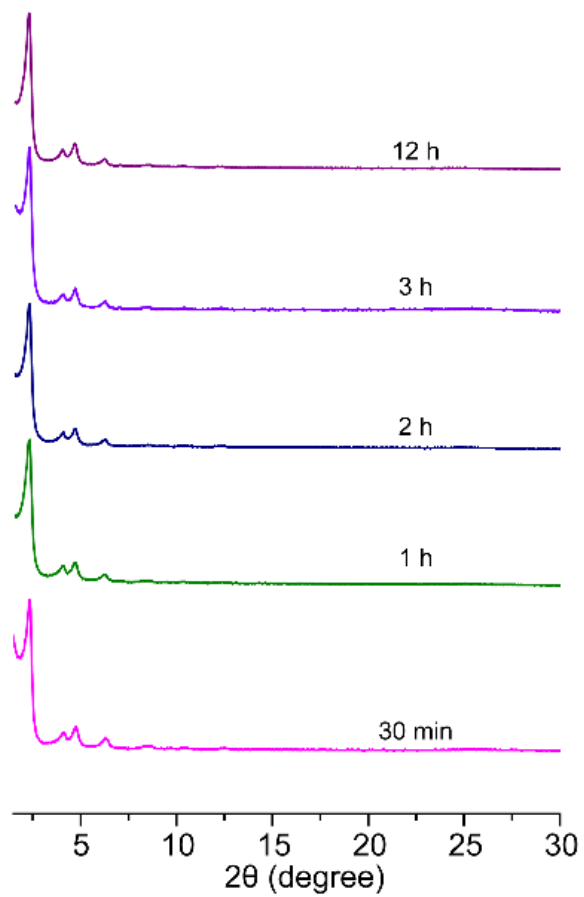


Fig. S7 Reaction-time-dependent PXRD patterns of Fe-COF_{TTA-BPA} synthesized under ambient conditions in dioxane/mesitylene (v/v = 1:1) with 6 M HOAc and Fe(OTf)₂.

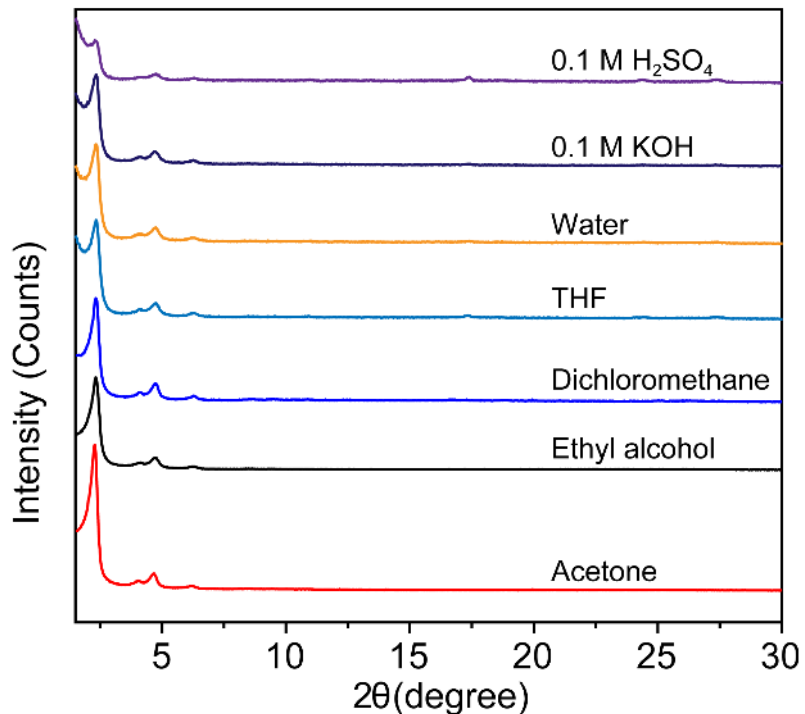


Fig. S8 Stability test of Fe-COF_{TTA-BPA} in various solvents and solutions. The stability tests were performed by mixing Fe-COF_{TTA-BPA} powders with various solvents and solutions for 72 h (3 days). The remained crystallinity of Fe-COF_{TTA-BPA} were evaluated by using PXRD intensity compared to their intrinsic counterparts.

S3.2 Crystal structure and stacking models

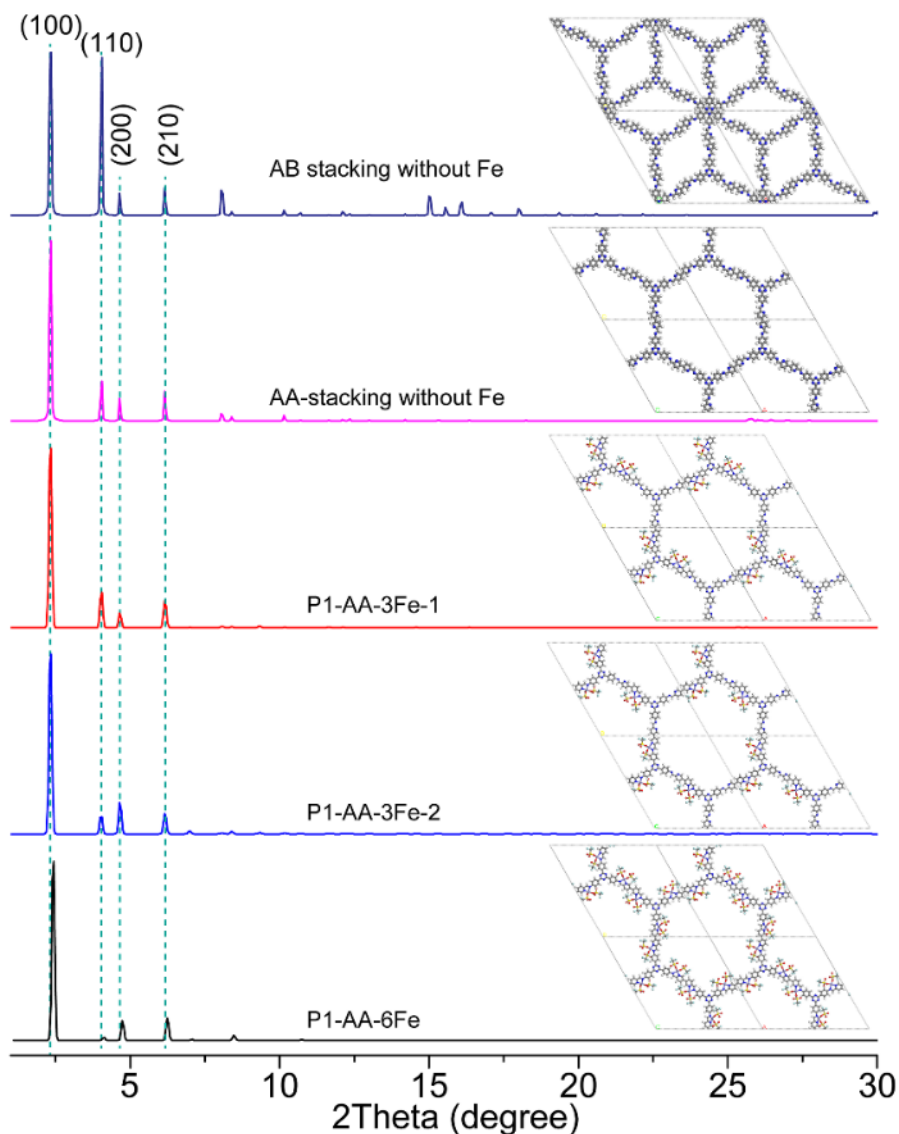


Fig. S9 Calculated PXRD patterns and corresponding topological structures for $\text{COF}_{\text{TTA-BPA}}$ and $\text{Fe-COF}_{\text{TTA-BPA}}$.

The main peaks slightly shift to higher diffraction angles due to the Fe(II) coordination compared to the simulated metal-free AA stacking modes (Fig. S9). The unit cell parameters for $\text{Fe-COF}_{\text{TTA-BPA}}$ are $a = 43.0198 \text{ \AA}$, $b = 43.9075 \text{ \AA}$, $c = 3.5249 \text{ \AA}$, $\alpha = \beta = 90^\circ$ and $\gamma = 120^\circ$ in $P1$ space group (P1-AA-6Fe model in Fig. S9) with good residual factors of $R_{wp} = 6.21\%$ and $R_p = 4.50\%$.

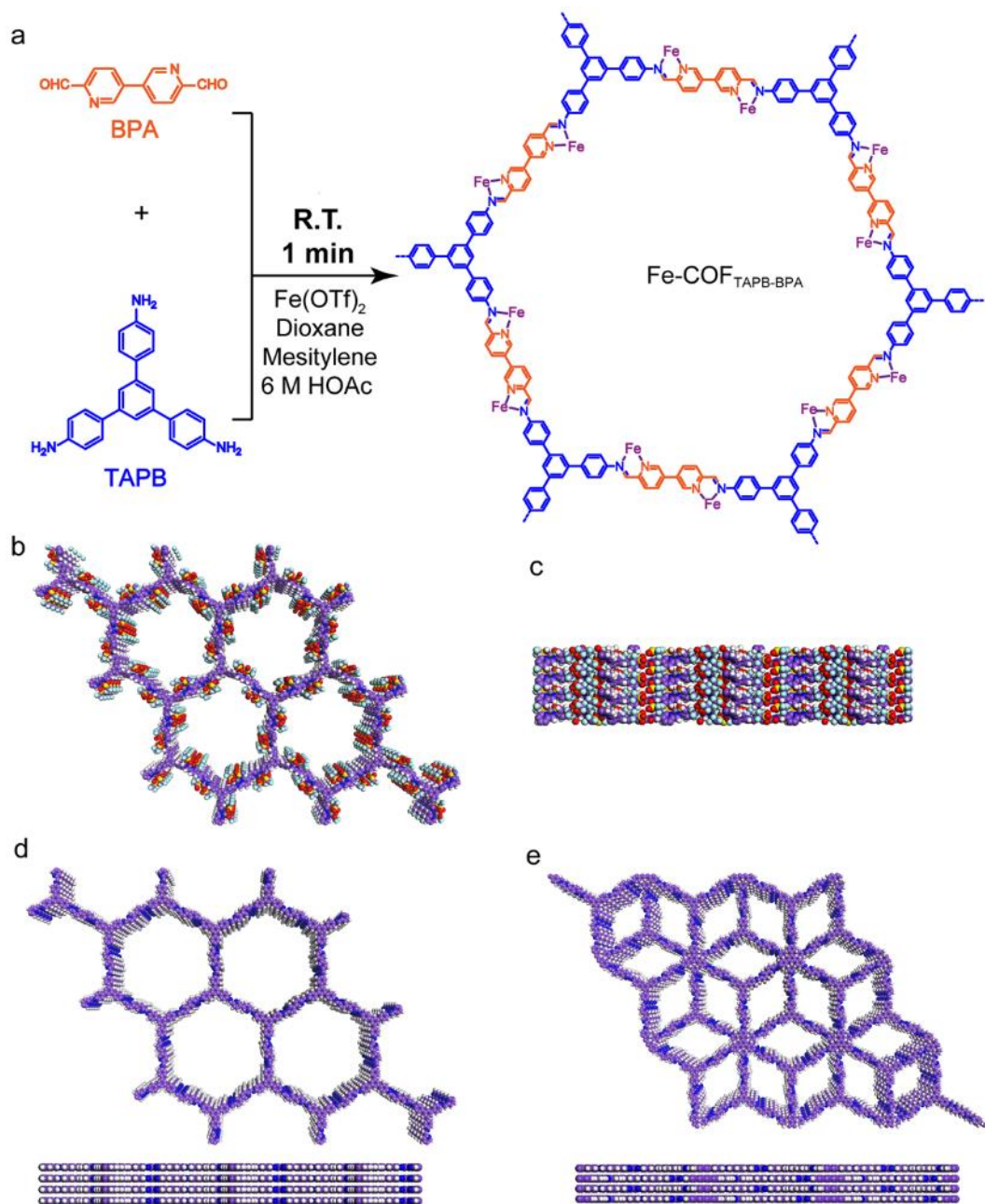


Fig. S10 (a) Schematic diagram of the structure of $\text{Fe-COF}_{\text{TAPB-BPA}}$ synthesized from TAPB and BPA. (b) Top-view and (c) cross-view topological structures of $\text{Fe-COF}_{\text{TAPB-BPA}}$ in AA stacking mode (P1), (d) $\text{COF}_{\text{TAPB-BPA}}$ in AA stacking mode (P6/m), and (e) $\text{COF}_{\text{TAPB-BPA}}$ in AB stacking mode (P63/m).

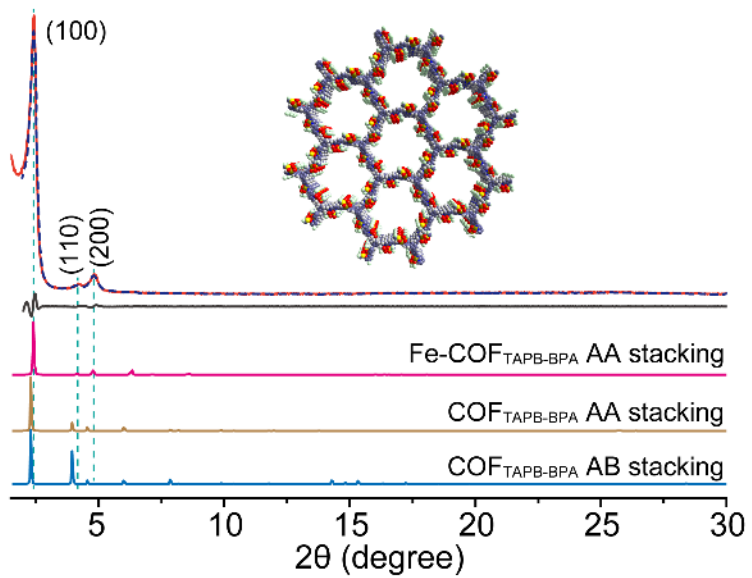


Fig. S11 Experimental and refined PXRD patterns of $\text{Fe-COF}_{\text{TAPB-BPA}}$. Insets: AA stacking models. The lattice parameters for $\text{Fe-COF}_{\text{TAPB-BPA}}$ are optimized as $a = 42.8224 \text{ \AA}$, $b = 43.5567 \text{ \AA}$, $c = 5.6515 \text{ \AA}$, $\alpha = \beta = 90^\circ$ and $\gamma = 120^\circ$ in $P1$ space group with the good residual factors of $R_{\text{wp}} = 6.95\%$ and $R_{\text{p}} = 5.22\%$.

S3.3 Morphologies

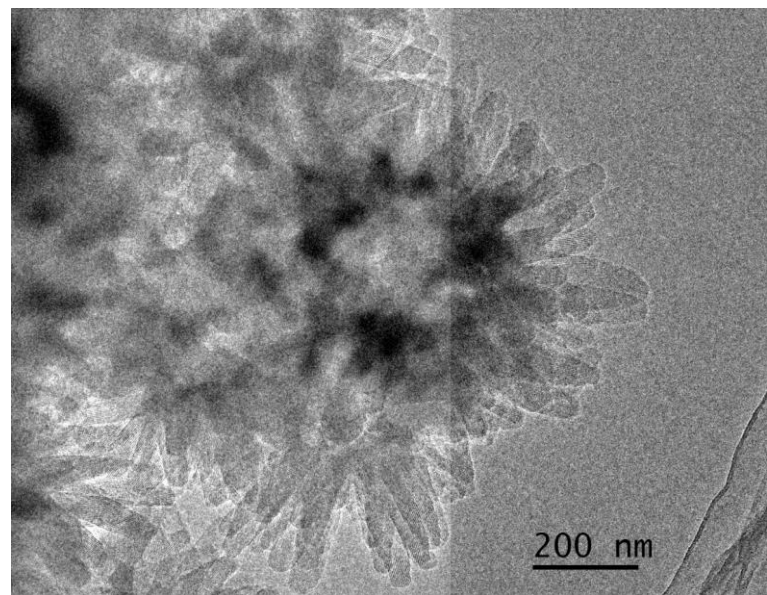


Fig. S12 TEM image of Fe-COF_{TTA-BPA} on large scale.

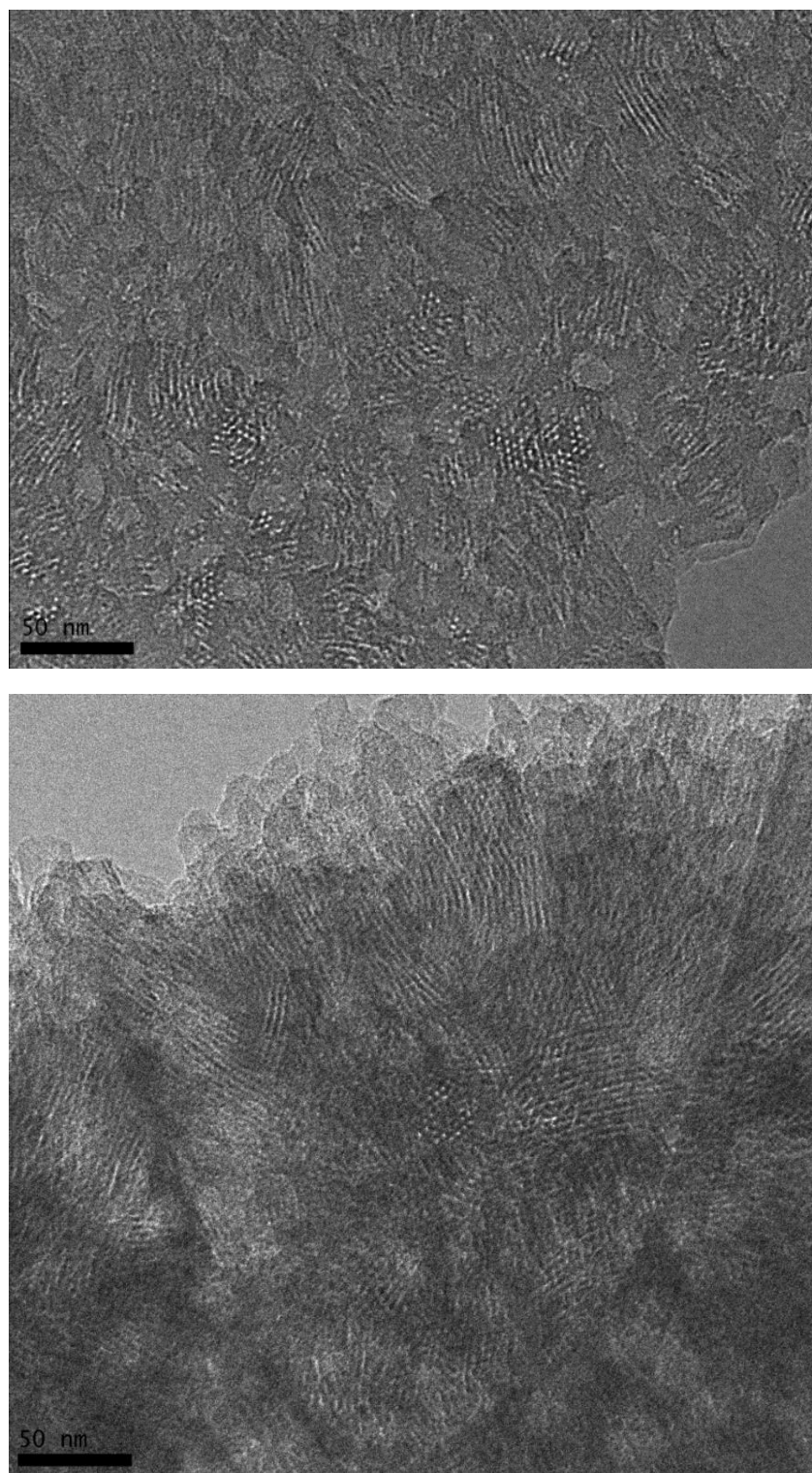


Fig. S13 TEM images of Fe-COF_{TAPB-BPA}.

S3.4. Isotherms and pore size distribution

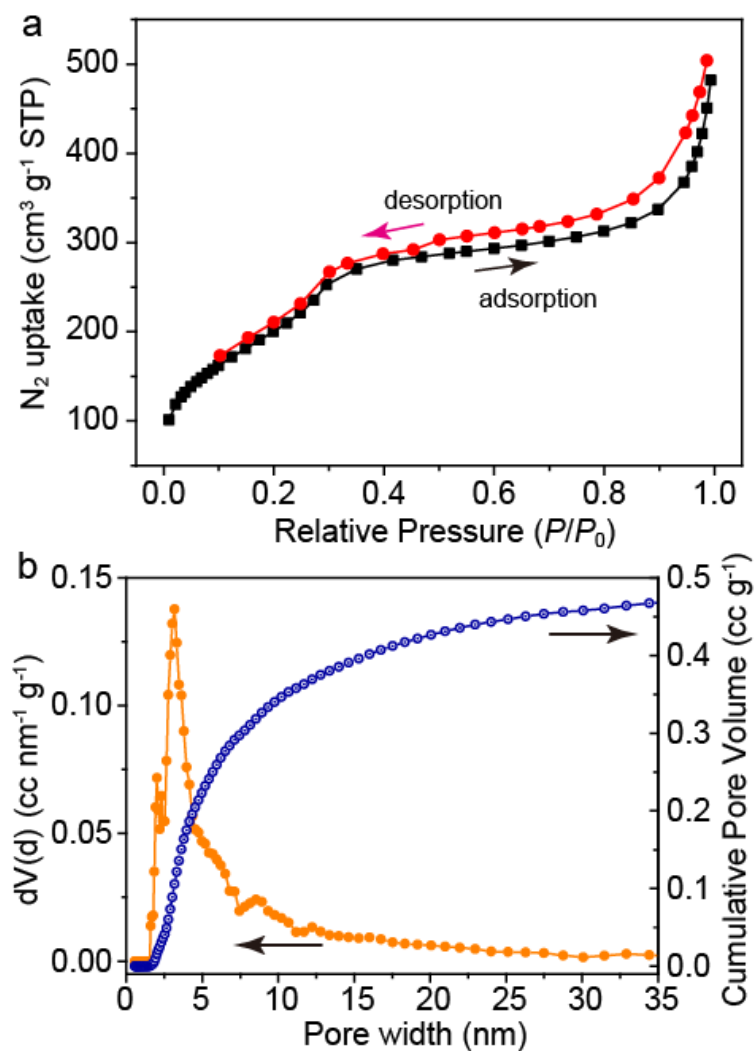


Fig. S14 (a) N_2 sorption-desorption isotherms at 77 K, (b) pore-size distribution and cumulative pore volume of Fe-COF_{TTA-BPA}.

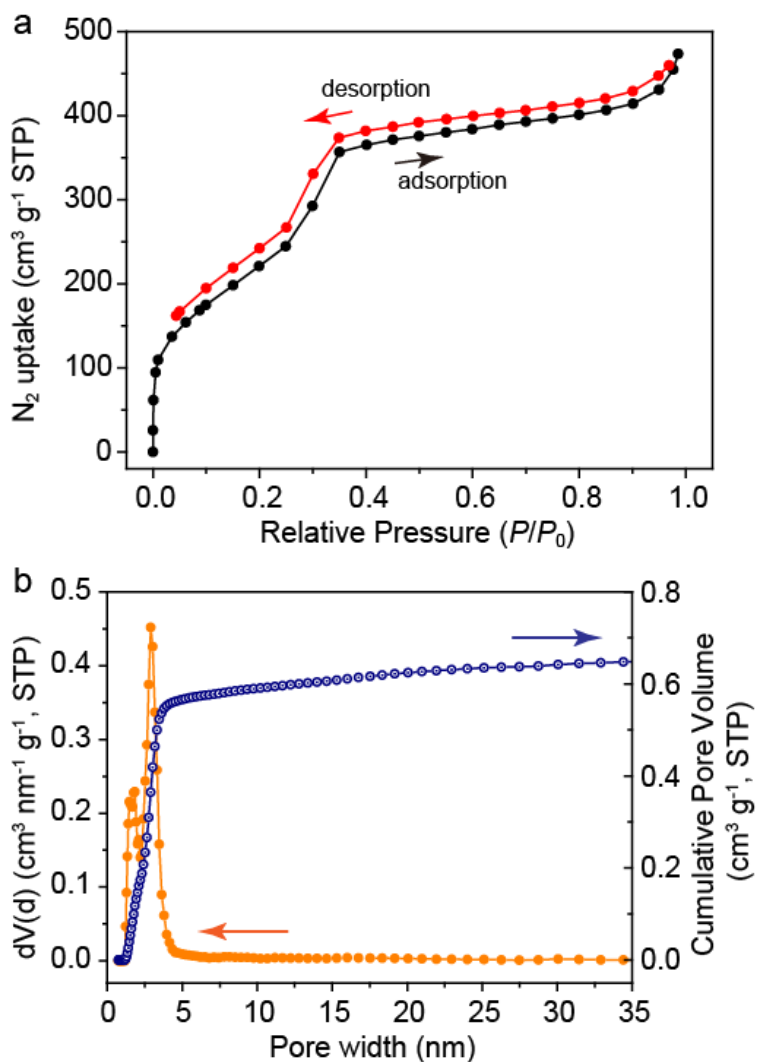


Fig. S15 (a) N_2 sorption-desorption isotherms at 77 K, (b) pore-size distribution and cumulative pore volume for Fe-COF_{TAPB-BPA}.

Table S1. Summary of experimental and calculated porous properties of BPA-based Fe-COFs.

Entry	Fe-COF _{TTA-BPA}	Fe-COF _{TAPB-BPA}
BET surface area ($\text{m}^2 \text{ g}^{-1}$)	809.16	928.37
Pore volume ($\text{cm}^3 \text{ g}^{-1}$)	Exp. 0.577	0.733
Cal. 0.592	0.777	
QSDFT	2.80	2.87
Pore size (nm)	TEM 2.85	2.92
Cal. 3.06		3.12

Notes: **Exp.** were experimental data evaluated from N2 sorption isotherms. **QSDFT** represented the values estimated from pore size distribution using quenched solid density function theory (QSDFT) model for cylindrical pores. **TEM** meant the measured pore sizes from TEM images. **Cal.** represented the values from theoretically predicted crystal structures.

S3.5 Solid-state ^{13}C NMR and FTIR spectra

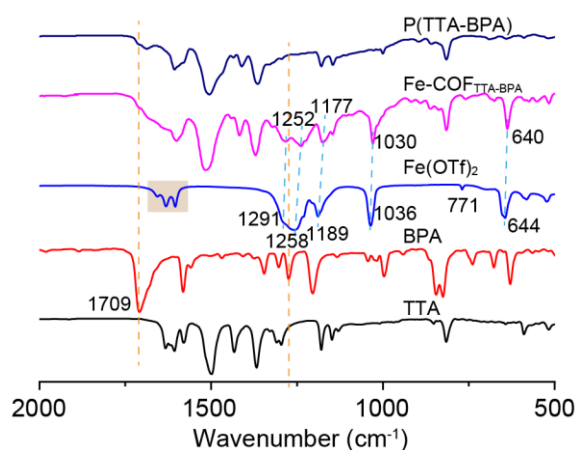


Fig. S16 FT-IR spectra for Fe-COF_{TTA-BPA}, P(TTA-BPA), Fe(OTf)₂, BPA and TTA.

We can observe OTf⁻ ligand in FT-IR spectra. The bands of OTf⁻ in Fe(OTf)₂ at 1291, 1258, 1189, 1036, 771 and 644 cm cm⁻¹ could be identified to the antisymmetric stretching vibration of the SO₃⁻ group [$\nu_{as}(SO_3^-)$], symmetric stretching vibration of the CF₃ group [$\nu_s(CF_3)$], antisymmetric stretching vibration of the CF₃ group [$\nu_{as}(CF_3)$], symmetric stretching vibration of the SO₃⁻ group [$\nu_s(SO_3^-)$], symmetric stretching $\nu_s(S-CF_3)$ and $\nu_s(C-SO_3)$ vibration, respectively.^[S5-S7] These characteristic bands were also found in the spectrum of Fe-COF_{TTA-BPA} with a slight shift to lower wavenumber due to the alternative environment of OTf⁻, which suggests possible coordination of Fe(II) to iminopyridine linkages in the Fe-COF_{TTA-BPA}.

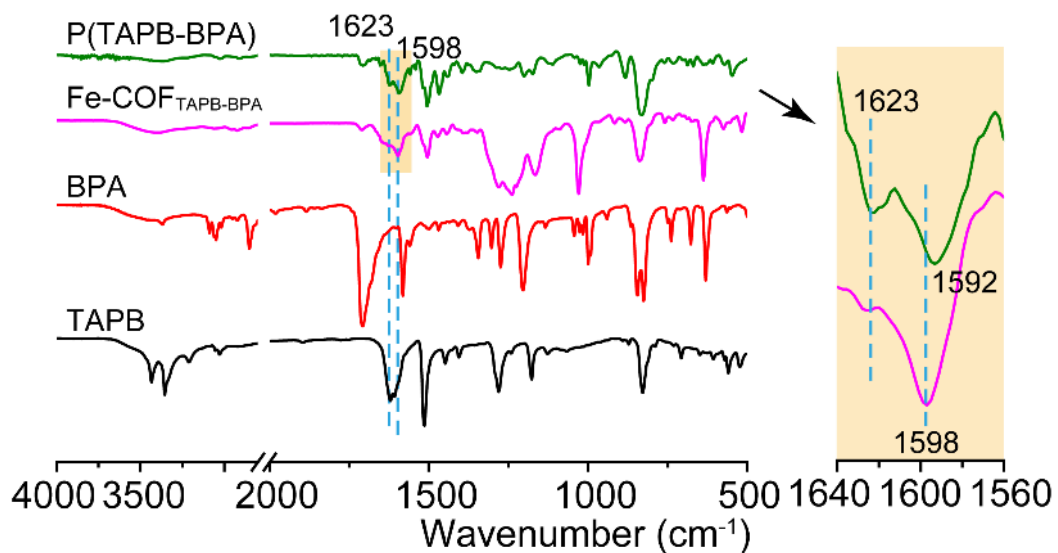


Fig. S17 FTIR spectra of Fe-COF_{TAPB-BPA} compared to amorphous P(TAPB-BPA), BPA, and TAPB. The total consumption of amine and most aldehyde groups is indicated as the disappeared N-H (around 3300 cm⁻¹) and C=O (~1709 cm⁻¹) stretching vibration modes

Table S2. Typical FTIR peaks of imine bond in Fe-COFs compared to amorphous powders without Fe(II).

Entry	P(TTA-BPA)	Fe-COF _{TTA-BPA}	P(TAPB-BPA)	Fe-COF _{TAPB-BPA}
Imine bond vibration				
	1623 cm ⁻¹	1597 cm ⁻¹	1623 cm ⁻¹	1598 cm ⁻¹

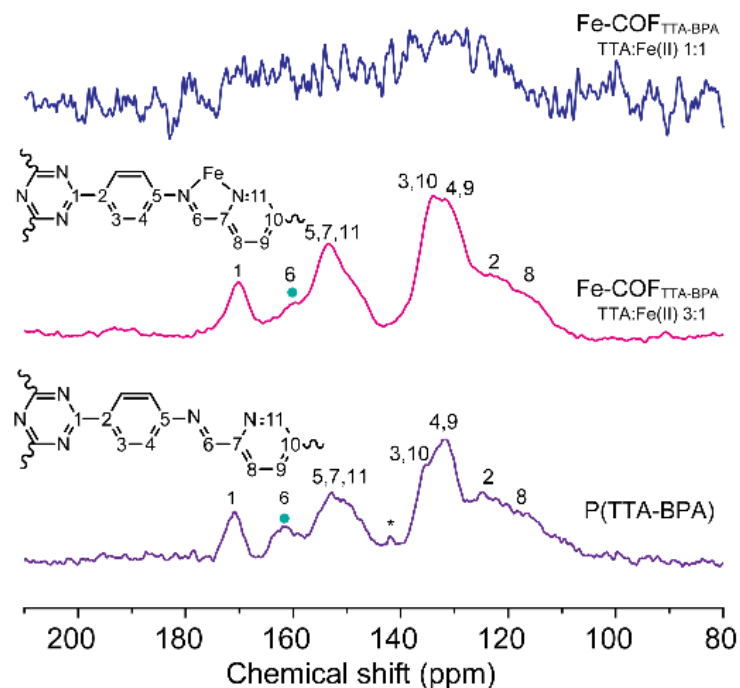


Fig. S18 Solid-state ¹³C-NMR spectra of Fe-COF_{TTA-BPA} compared to P(TTA-BPA).

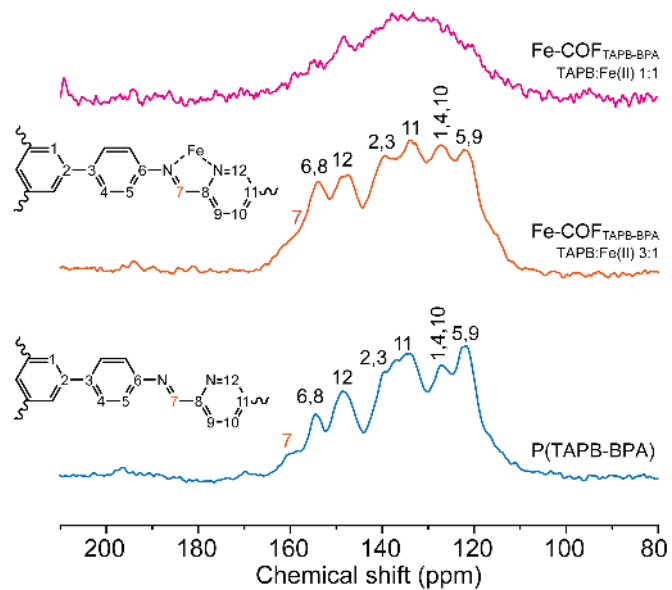


Fig. S19 Solid-state ^{13}C -NMR spectra of $\text{Fe-COF}_{\text{TAPB-BPA}}$ compared to P(TAPB-BPA).

Table S3. Typical solid-state ^{13}C -NMR peaks of imine bond in Fe-COFs compared to amorphous powders without Fe(II).

Entry	Imine bond	Imine bond coordinating to Fe(II)
P(TTA-BPA)	161.40 ppm	/
$\text{Fe-COF}_{\text{TTA-BPA}}$	/	159.70 ppm
Model Compd. 1	161.76 ppm	/
[Fe-1](OTf) ₈	/	159.04 ppm
[Fe-2](OTf) ₈	/	158.61 ppm
P(TAPB-BPA)	159.98 ppm	/
$\text{Fe-COF}_{\text{TAPB-BPA}}$	/	159.03 ppm

The typical ^{13}C NMR signals of Fe-COFs were detected when the molar ratio of TTA/TAPB to $\text{Fe}(\text{OTf})_2$ was set as 3:1. The ratio of signal-to-noise for $\text{Fe-COF}_{\text{TTA-BPA}}$ with the molar ratio of TTA: $\text{Fe}(\text{OTf})_2$ as 1:1 was poor due to the presence of magnetic $\text{Fe}(\text{II})$.

As summarized in Table S3, the chemical shifts of metal-free imine C is around 161.4 ppm for the solid-state ^{13}C -NMR spectra of polymers and metal-free model compounds. In Fe-COFs, the chemical shift of imine C is around 159 ppm in, similar to the model complexes $[\text{Fe-1}](\text{OTf})_8$ and $[\text{Fe-2}](\text{OTf})_8$ due to the coordination of Fe to iminopyridine moieties.

S3.6 XPS spectra

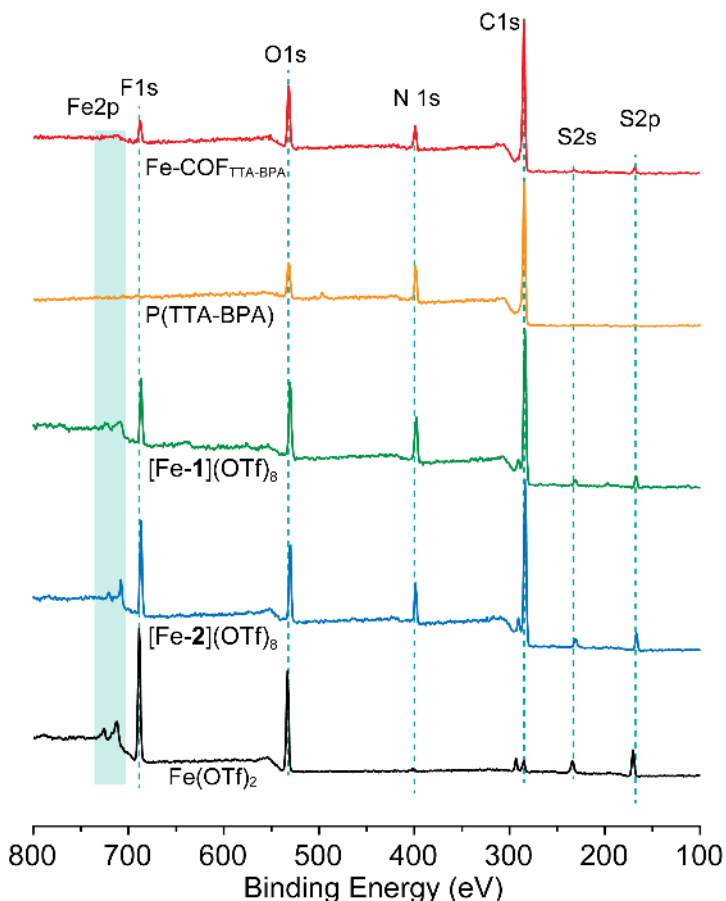


Fig. S20 XPS survey curves of $\text{Fe-COF}_{\text{TTA-BPA}}$, $\text{P}(\text{TTA-BPA})$, $[\text{Fe-1}](\text{OTf})_8$, $[\text{Fe-2}](\text{OTf})_8$, and $\text{Fe}(\text{OTf})_2$.

The survey spectra indicate the existence of Fe species in Fe-COFs similar to Fe-involved model complexes. The survey spectra also prove the existence of OTf^- in $\text{Fe-COF}_{\text{TTA-BPA}}$ indicated by the typical peaks of F1s, S2p and S2s in survey spectra.

The final content of the Fe element is ~7.2 wt.% in BPA-based Fe-COFs quantified by using inductively coupled plasma-atomic emission spectrometry (ICP-AES) are comparable to the calculated content of Fe in lattice 9.96 wt.%.

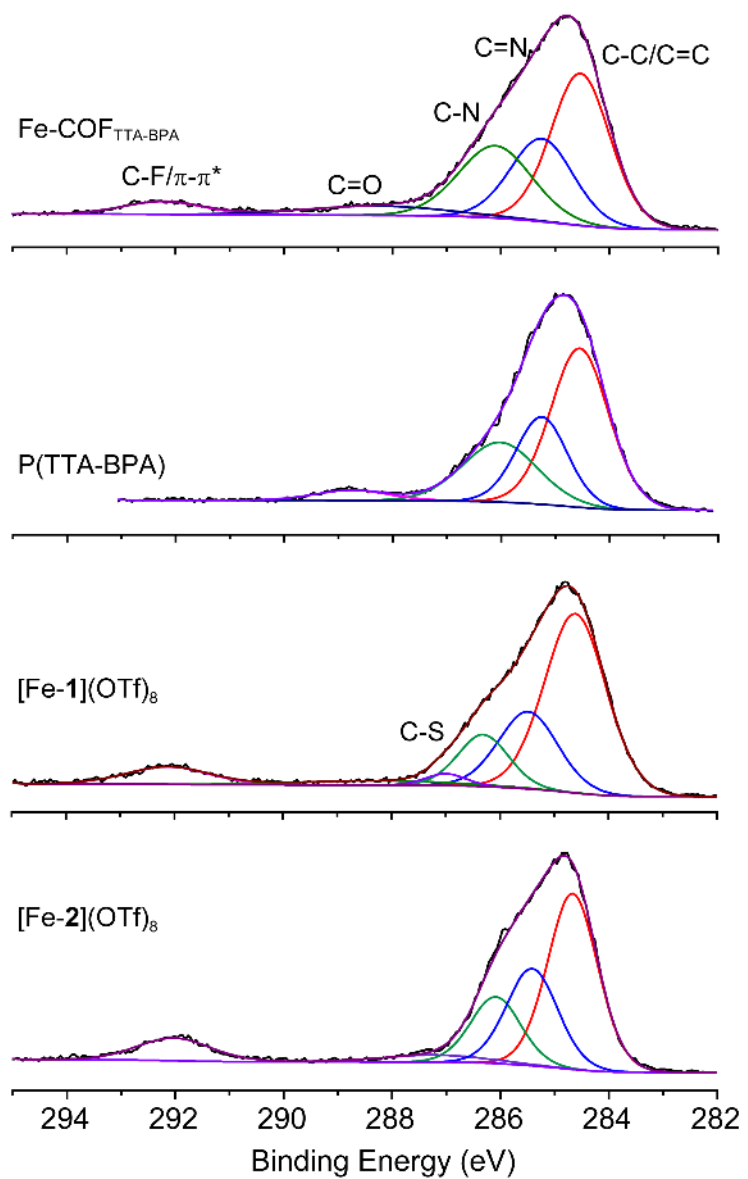


Fig. S21 High-resolution XPS spectra of C1s for Fe-COF_{TTA-BPA}, amorphous P(TTA-BPA), [Fe-1](OTf)₈ and [Fe-2](OTf)₈. High-resolution C1s spectra of Fe-COF_{TTA-BPA} show similar peak shape and assignments with [Fe-1](OTf)₈ due to the similar building blocks.

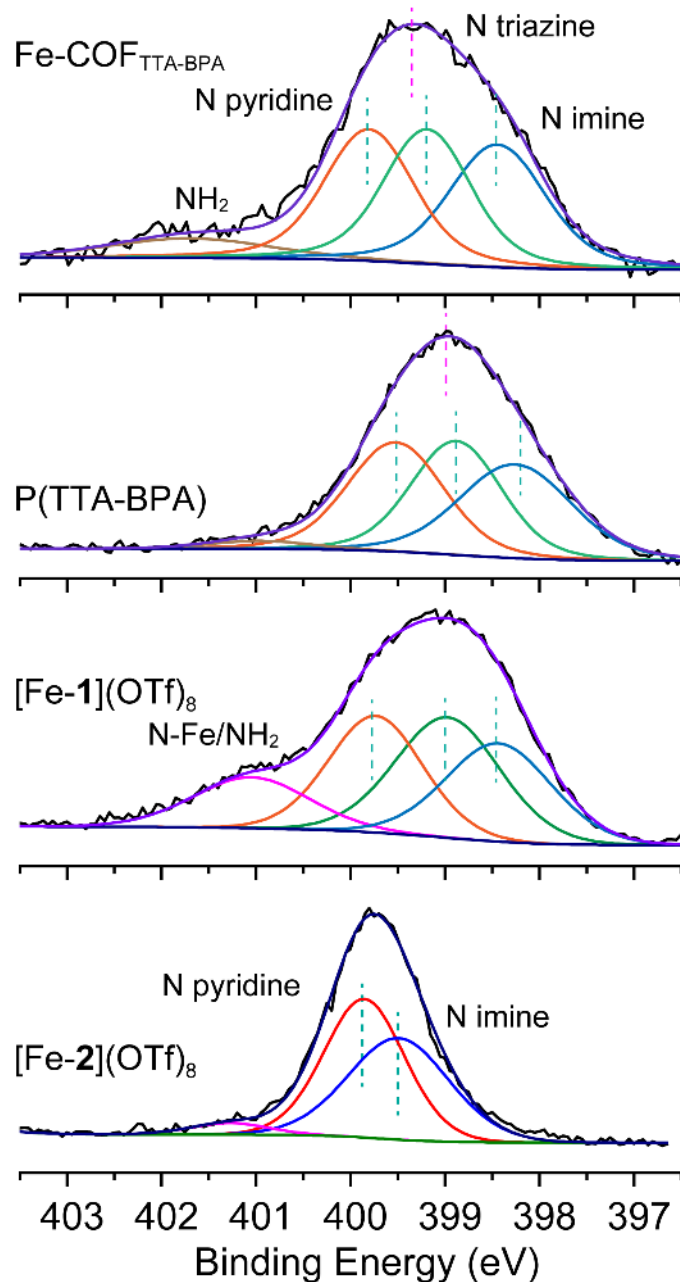


Fig. S22 High-resolution XPS spectra of N1s for Fe-COF_{TTA-BPA}, P(TTA-BPA), [Fe-1](OTf)₈, and [Fe-2](OTf)₈.

Table S4. Binding energy of N1s peaks for Fe-COF_{TTA-BPA} compared to P(TTA-BPA).

Entry	N1s main peak	pyridinic N	imine N	triazine N
Fe-COF _{TTA-BPA}	399.34 eV	399.83 eV	399.22 eV	398.42 eV
P(TTA-BPA)	398.97 eV	399.53 eV	398.90 eV	398.26 eV
ΔE_{BE}	0.37 eV	0.30 eV	0.32 eV	0.16 eV

Notes: ΔE_{BE} represents the difference of various N binding energy between Fe-COF_{TTA-BPA} and P(TTA-BPA).

High-resolution N1s spectra of Fe-COF_{TTA-BPA} show comparable peak shape and assignments with [Fe-1](OTf)₈ due to the similar building blocks. The N1s cores of Fe-COFs can be assigned to pyridine N, imine N, and triazine N according to the molecular structure. As shown in Table S4, these assignment binding energies are higher than that in P(TTA-BPA) with a difference of $\Delta E = 0.37$ eV. The binding energy shifts are largely attributed to the changes of pyridine N and imine N due to the electron donation from N groups to metal ions.

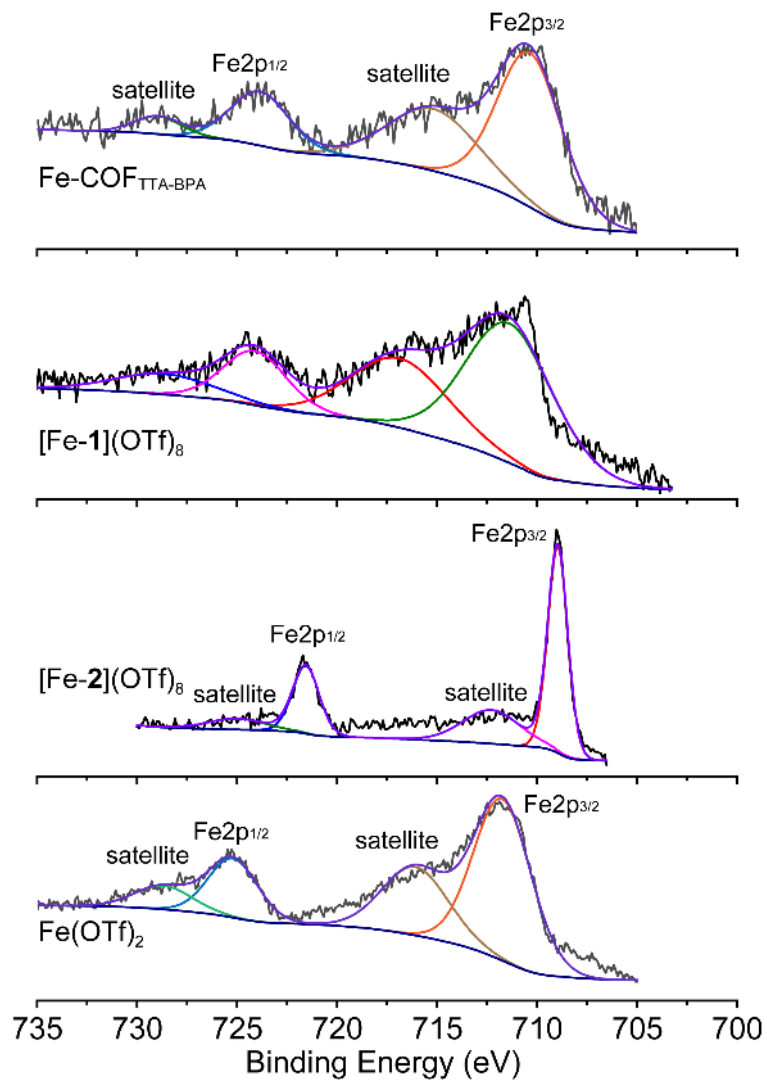


Fig. S23 High-resolution XPS spectra of Fe2p for Fe-COF_{TTA-BPA}, P(TTA-BPA), [Fe-1](OTf)₈, and [Fe-2](OTf)₈.

Table S5. The binding energy of Fe2p peaks for Fe-COF_{TTA-BPA} compared to Fe-model complexes and Fe(OTf)₂.

Entry	Fe 2p _{3/2}	satellite 1	Fe 2p _{1/2}	satellite 2
Fe-COF _{TTA-BPA}	710.34 eV	715.74 eV	723.82 eV	728.94 eV
[Fe-1](OTf) ₈	710.23 eV	716.09 eV	723.54 eV	728.73 eV
[Fe-2](OTf) ₈	708.97 eV	712.37 eV	721.59 eV	725.34 eV
Fe(OTf) ₂	711.87 eV	716.25 eV	725.29 eV	728.92 eV

Two splitting spin-orbit of Fe2p scans for Fe-COF_{TTA-BPA} are assigned to 2p_{3/2} at 710.34 eV and 2p_{1/2} at 723.82 eV with two satellite peaks at 715.74 and 728.94 eV. These assignments are essentially following that of the model [Fe-1](OTf)₈ but a slightly higher binding energy (Table S5). These results indicate the Fe(II) coordination to iminopyridine N atoms in Fe-COF_{TTA-BPA} similar to the metal-ligand interaction in [Fe-1](OTf)₈.

S3.7 EXAFS fitting

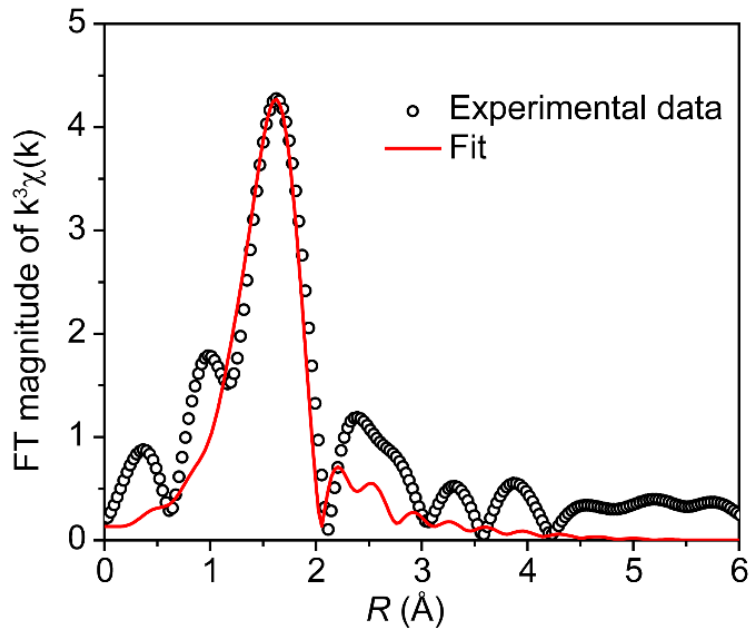


Fig. S24 EXAFS curve fitting for Fe-COF_{TTA-BPA}

Table S6. EXAFS curve fitting parameters of Fe-COF_{TTA-BPA}.

Shell	N	R (Å)	σ^2 (10^{-3}\AA^2)	ΔE_0 (eV)	S_0^2
Fe-O	2.0	1.97700	8.00	-1.000	1.000
Fe-N	2.0	2.11260	5.00	1.000	1.150

Notes: N , coordination number; R , the distance between absorber and backscatter atoms; σ^2 , Debye-Waller factor to account for both thermal and structural disorders; ΔE_0 , inner potential correction; S_0^2 , the amplitude reduction factor, which was initially fixed to 0.97 as determined from Fe foil fitting. Error bounds (accuracies) that characterize the structural parameters obtained by EXAFS spectroscopy were estimated as $N \pm 20\%$; $R \pm 1\%$; $\sigma^2 \pm 20\%$; $\Delta E_0 \pm 20\%$.

S3.8 Magnetic properties

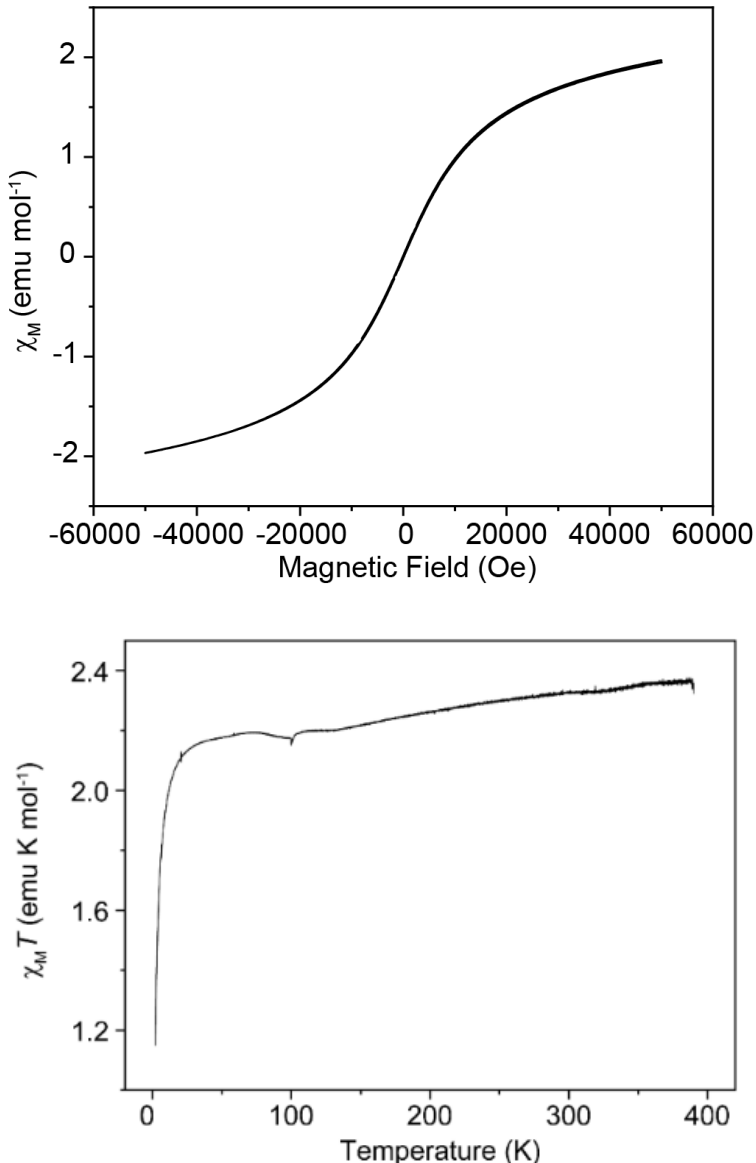


Fig. S25 Magnetization curve at 2 K (upper) and $\chi_M T$ vs. T plot for Fe-COF_{TTA-BPA} (bottom).

The S-shape magnetization curve shows that the χ_M symmetrically quasi-linearly increases with the enhanced magnetic field to ± 10 kOe and tends to saturate under the magnetic field higher than ± 30 kOe, implying the paramagnetic performance of Fe-COF_{TTA-BPA}. The sectionalized change is illustrated in the $\chi_M T \sim T$ and $\chi_M \sim T$ plots. The

χ_M slightly increases as the temperature decreased from 300 K to around 25 K, followed by a sharp increase to 0.57 emu mol⁻¹ and leveling off until 2 K. The effective magnetic moment (μ_{eff}) is evaluated as $4.31\mu_B$ from $\chi_M \sim T$ fitting based on Currie-Weiss theory. The total spin angular momentum is calculated as *ca.* 2.

S4. Control experiments

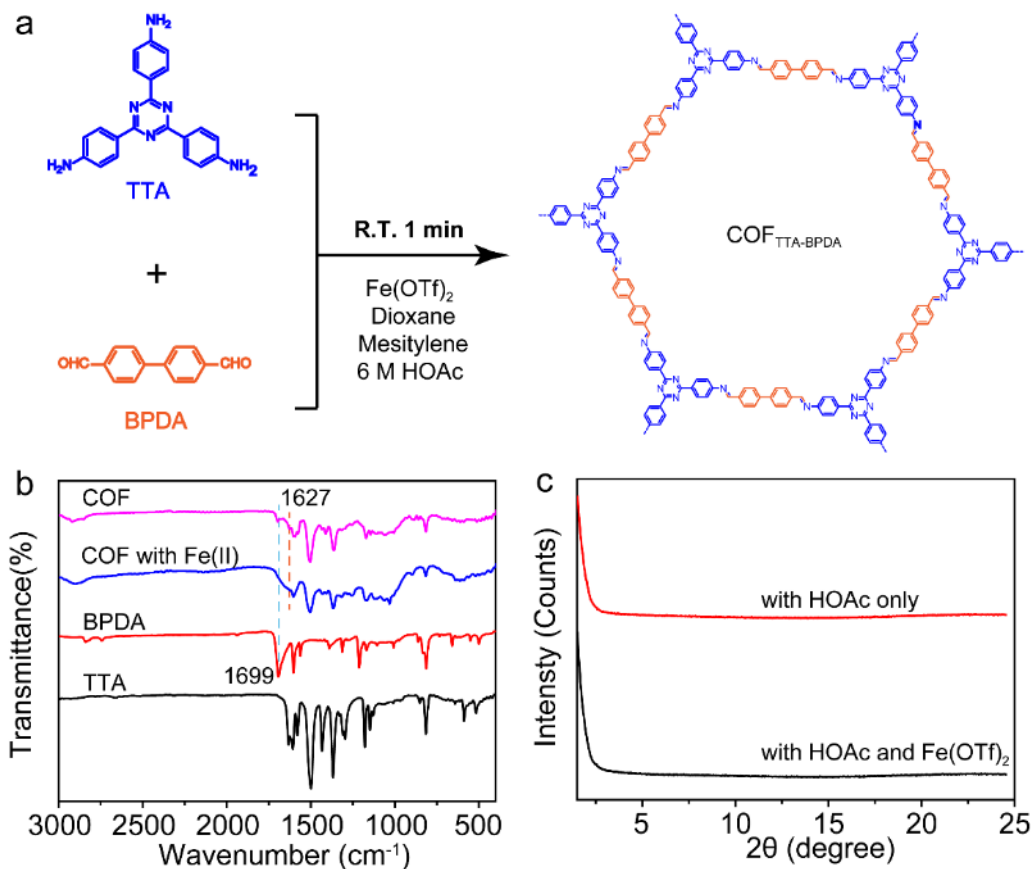


Fig. S26 (a) Schematic diagram of COF_{TTA-BPDA} constructed from TTA and BPDA at ambient conditions catalyzed with 6 M HOAc in the mixed solvent of dioxane and mesitylene (v:v = 1:1). (b) FTIR spectra of “COF_{TTA-BPDA}” with or without Fe(OTf)₂ compared to the corresponding building blocks. (c) PXRD patterns of “COF_{TTA-BPDA}” synthesized with or without Fe(OTf)₂.

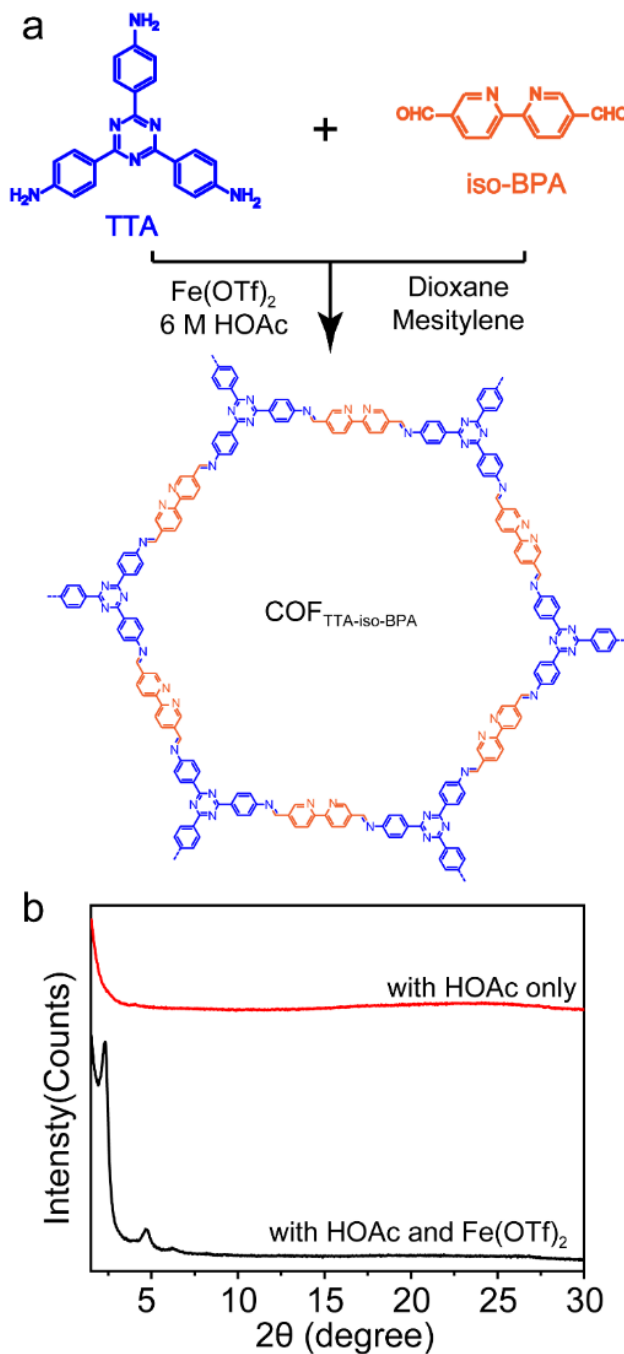


Fig. S27 (a) Schematic diagram of $\text{COF}_{\text{TTA-iso-BPDA}}$ constructed from TTA and iso-BPA under ambient conditions and (b) PXRD patterns of $\text{COF}_{\text{TTA-BPDA}}$ synthesized with or without $\text{Fe}(\text{OTf})_2$ catalyzed in the presence of 6 M HOAc in the mixed solvent of dioxane and mesitylene ($v:v = 1:1$).

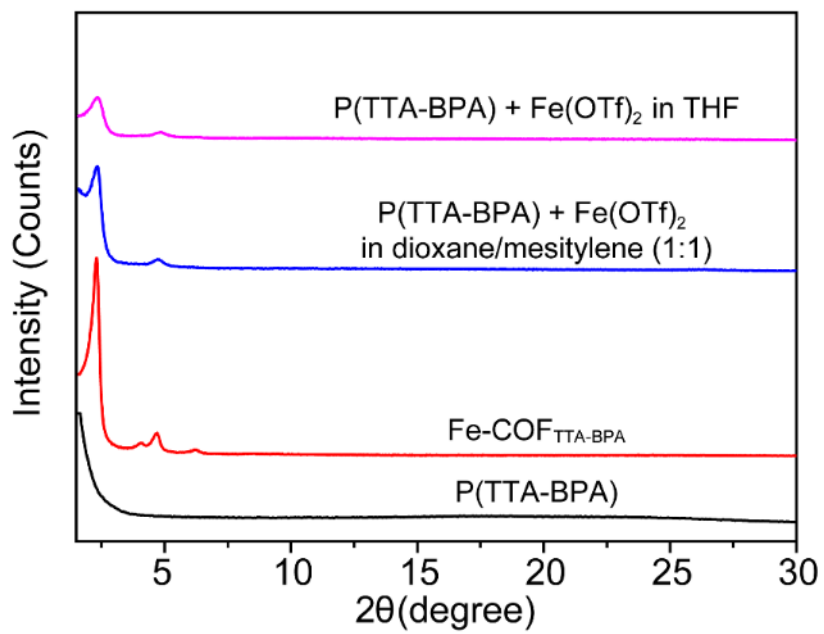


Fig. S28. Compared PXRD patterns of post-transferred crystalline Fe-COF_{TTA-BPA} from corresponding amorphous P(TTA-BPA) with the addition of Fe(OTf)₂ in different organic solvents to Fe-COF_{TTA-BPA} and P(TTA-BPA).

S5. Synthesis and characterization of PDA-based Fe-COFs.

S5.1 Crystalline structure and stacking models

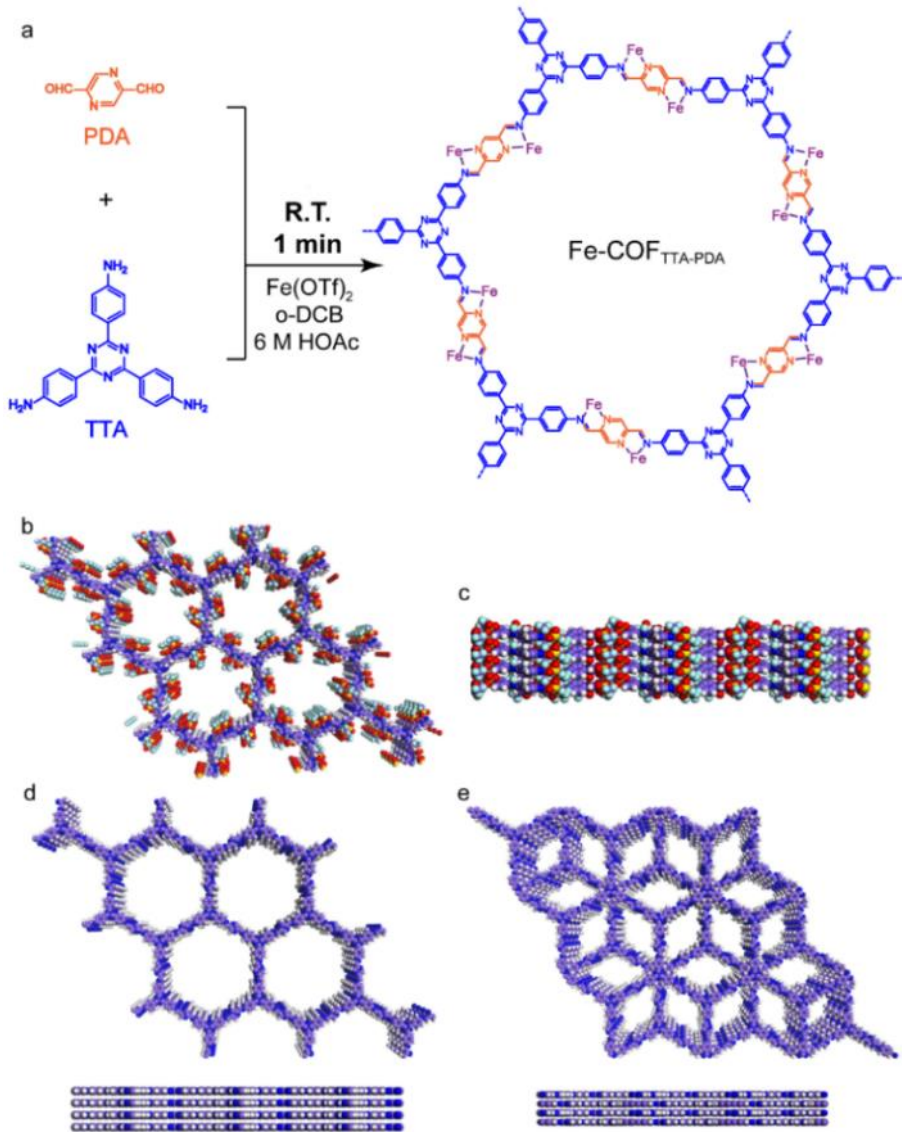


Fig. S29 (a) Schematic diagram of the structure of Fe-COF_{TTA-PDA} from TTA and PDA.

(b) Top-view and (c) cross-view topological structures of Fe-COF_{TTA-PDA} in AA stacking mode (P1), (d) COF_{TTA-PDA} in AA stacking mode (P6/m), and (e) COF_{TTA-PDA} in AB stacking mode (P63/m). The calculated crystal lattice values are $a = 37.4706 \text{ \AA}$, $b = 35.8836 \text{ \AA}$, $c = 4.0774 \text{ \AA}$, $\alpha = \beta = 90^\circ$ and $\gamma = 120^\circ$ ($R_{wp} = 5.39\%$ and $R_p = 4.40\%$) for Fe-COF_{TTA-PDA}.

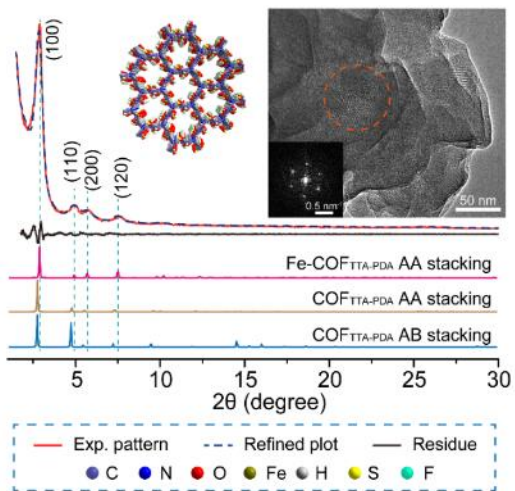


Fig. S30 Experimental and refined PXRD patterns of $\text{Fe-COF}_{\text{TTA-PDA}}$. Insets: the corresponding topological models in AA stacking, TEM image, and FFT pattern.

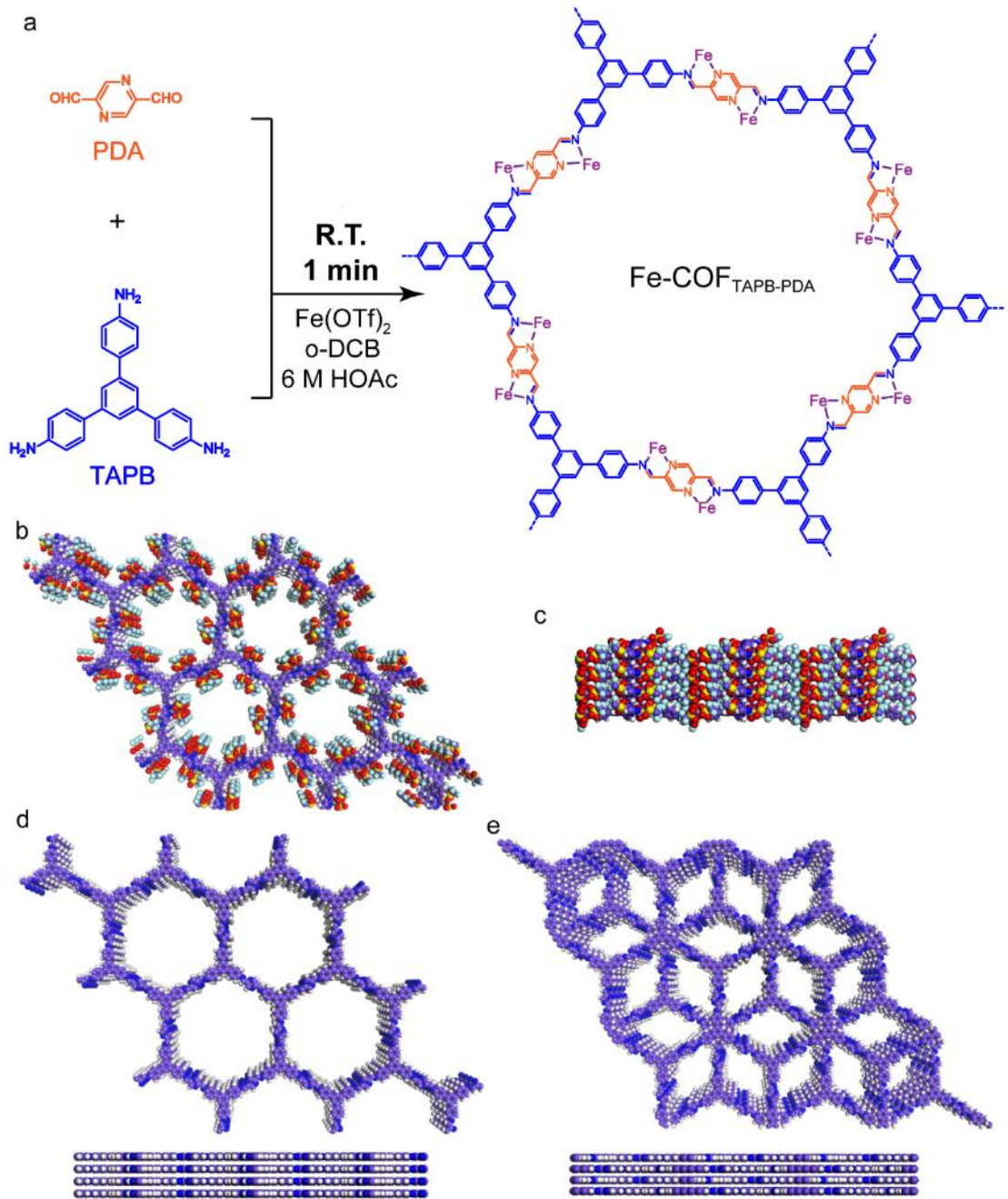


Fig. S31 (a) Schematic diagram of the structure of Fe-COF_{TAPB-PDA} synthesized from TAPB and PDA. (b) Top-view and (c) cross-view topological structures of Fe-COF_{TAPB-PDA} in AA stacking mode (P1), (d) COF_{TAPB-PDA} in AA stacking mode (P6/m), and (e) COF_{TAPB-PDA} in AB stacking mode (P63/m). The calculated crystal lattice values are $a = 36.2722 \text{ \AA}$, $b = 35.7041 \text{ \AA}$, $c = 5.1475 \text{ \AA}$, $\alpha = \beta = 90^\circ$ and $\gamma = 120^\circ$ ($R_{\text{wp}} = 4.80\%$ and $R_{\text{p}} = 3.89\%$) for Fe-COF_{TAPB-PDA}.

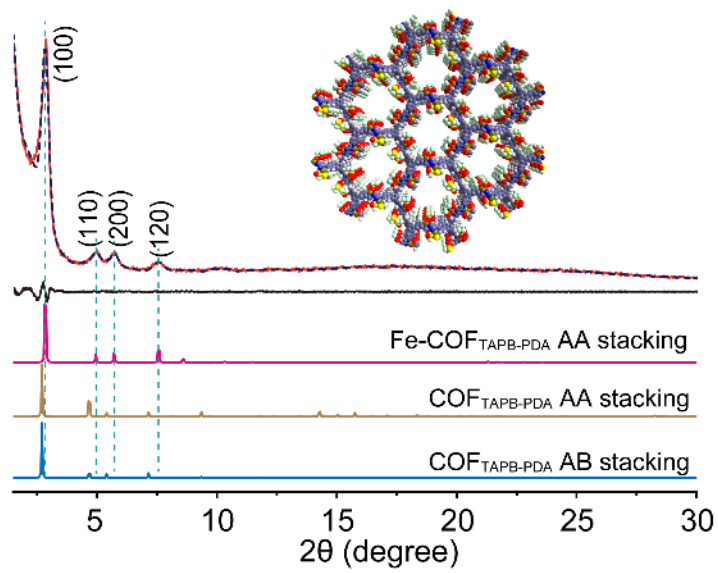


Fig. S32 Experimental and refined PXRD patterns of Fe-COF_{TAPB-PDA}. Insets: the corresponding topological models in AA stacking. The calculated PXRD patterns based on the eclipsed stacking mode with Fe(II)-iminopyrazine linkages after Pawley refinement well match with the experimental data

S5.2 TEM and HAADF-STEM images

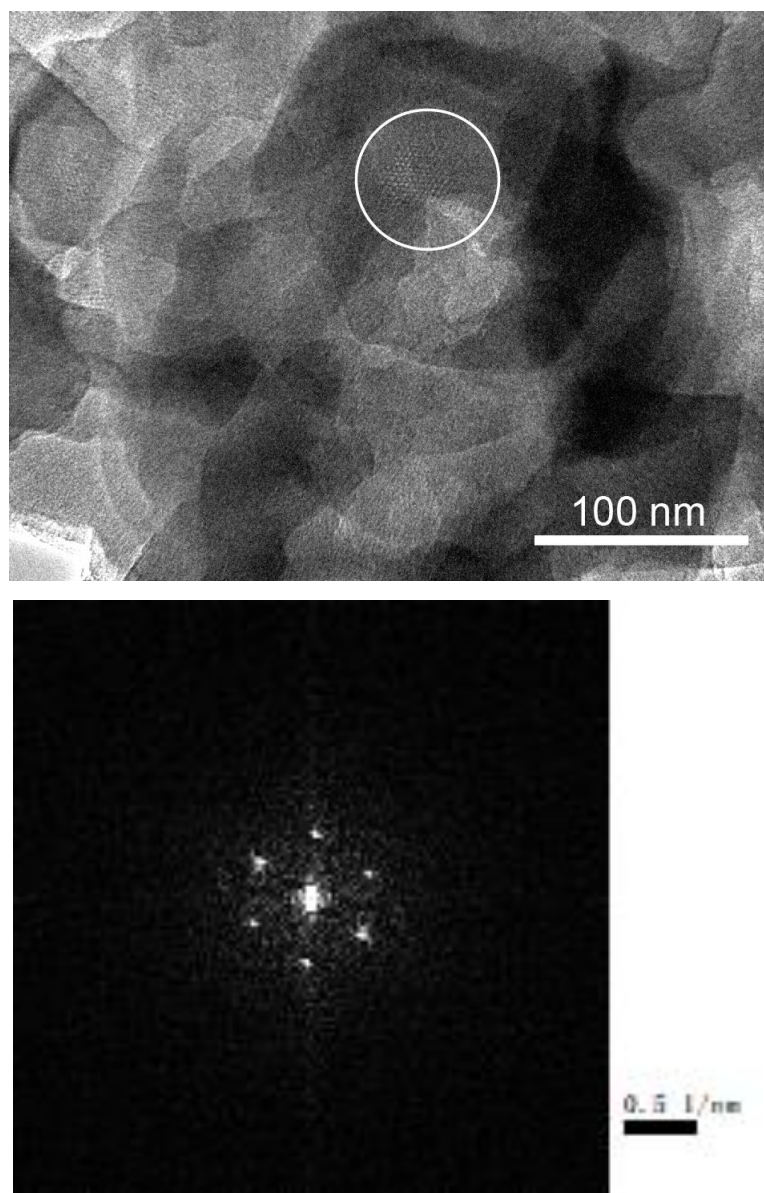


Fig. S33 TEM (upper) images of Fe-COF_{TAPB-PDA}. Obvious and ordered porous structures could be found in the white circle in the TEM image. The corresponding FFT pattern was presented at the bottom.

The pore sizes are measured as 2.19 ± 0.03 nm for Fe-COF_{TTA-PDA} and 2.06 ± 0.05 nm for Fe-COF_{TAPB-PDA}

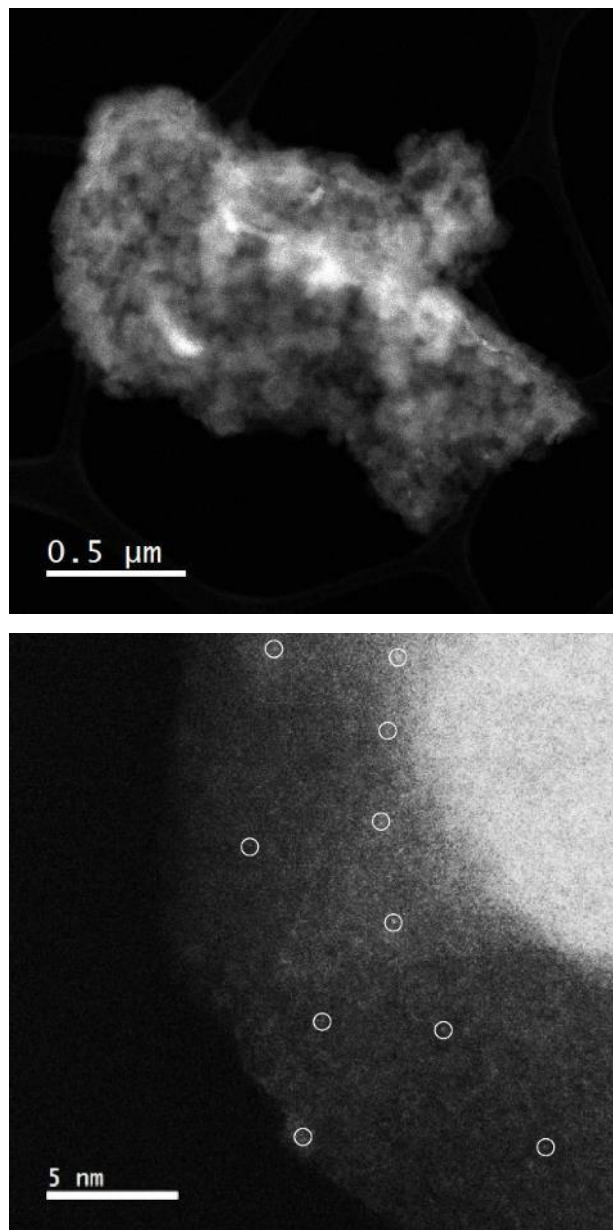


Fig. S34 HAADF-STEM and high-resolution STEM images of Fe-COF_{TTA-PDA}.

S5.3 Isotherms and pore size distribution of Fe-COFs

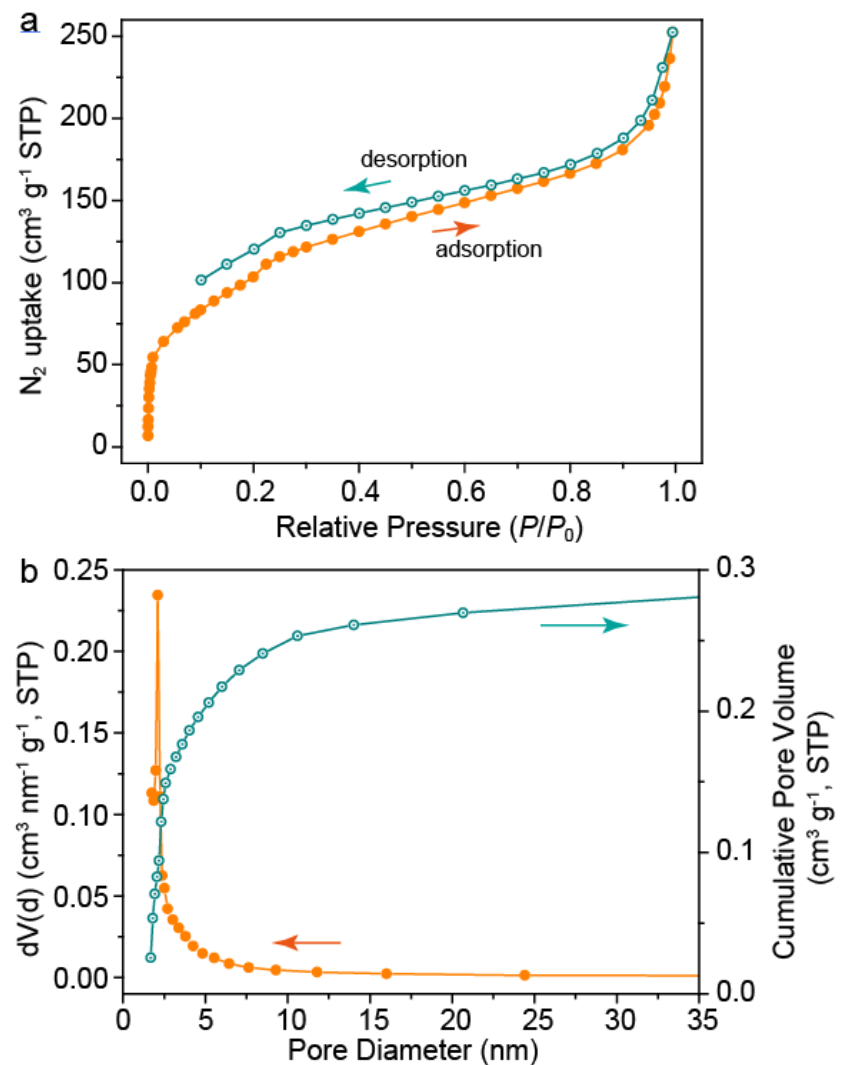


Fig. S35 (a) N_2 sorption-desorption isotherms at 77 K, (b) pore-size distribution and cumulative pore volume for Fe-COF_{TTA-PDA}.

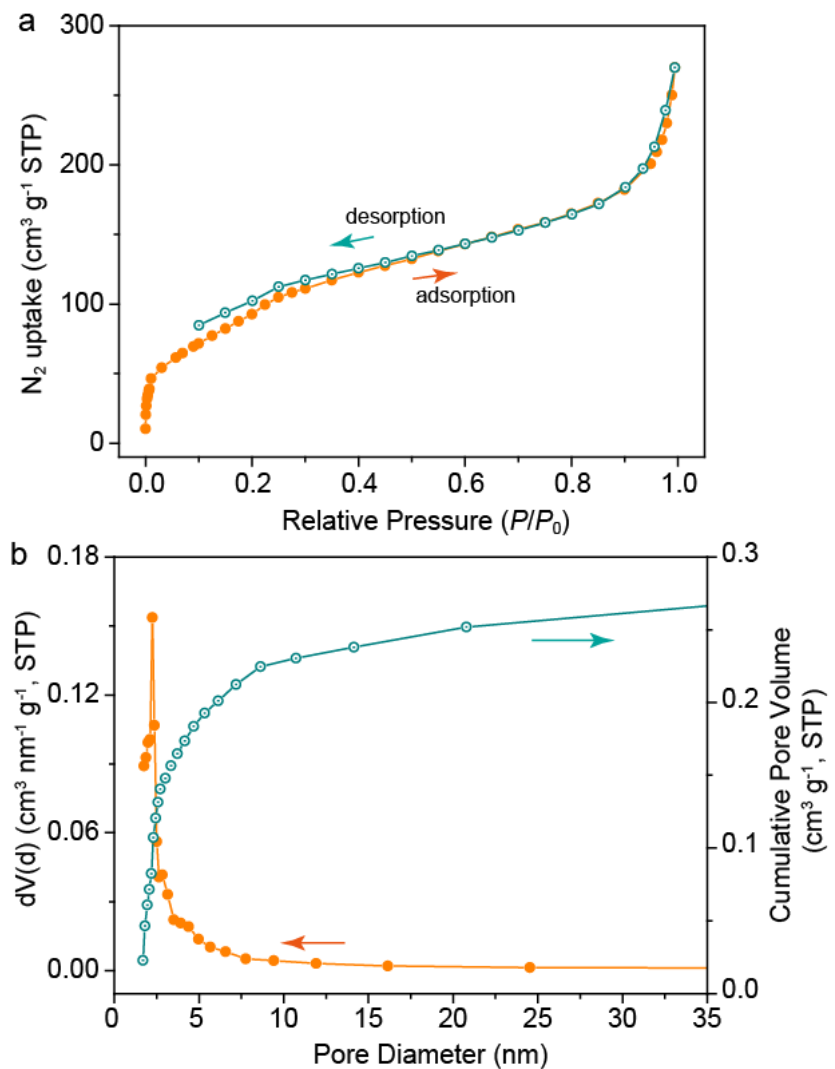


Fig. S36 (a) N_2 sorption/desorption isotherms at 77 K, (b) pore size distribution and cumulative pore volume for Fe-COF_{TAPB-PDA}.

Type-I isotherms are recorded to the microporosity nature of iminopyrazine-based Fe-COFs due to Fe coordination. Their BET surface areas are calculated as 403.31 m² g⁻¹ and 371.53 m² g⁻¹ for Fe-COF_{TTA-PDA} and Fe-COF_{TAPB-PDA}, respectively.

Table S7. Summary of experimental and calculated porous properties of PDA-based Fe-COFs.

Entry	Fe-COF _{TTA-PDA}	Fe-COF _{TAPB-PDA}
BET surface area ($\text{m}^2 \text{ g}^{-1}$)	403.31	371.53
Pore volume ($\text{cm}^3 \text{ g}^{-1}$)	Exp. 0.371 Cal. 0.375	0.282 0.261
QSDFT	2.12	2.08
Pore size (nm)	TEM 2.19 Cal. 2.24	2.06 2.16

Notes: **Exp.** were experimental data evaluated from N2 sorption isotherms. **QSDFT** represented the values estimated from pore size distribution using quenched solid density function theory (QSDFT) model for cylindrical pores. **TEM** meant the measured pore sizes from TEM images. **Cal.** represented the values from theoretically predicted crystal structures.

For the iminopyrazine-derived Fe-COFs, the pore sizes and pore volumes are 2.12 nm and $0.371 \text{ cm}^3 \text{ g}^{-1}$ for Fe-COF_{TTA-PDA}, 2.08 nm and $0.282 \text{ cm}^3 \text{ g}^{-1}$ for Fe-COF_{TAPB-PDA} by using quenched solid density function theory (QSDFT) model for cylindrical pores. These pore sizes are close to the 2.19 nm for Fe-COF_{TTA-PDA} and 2.06 nm for Fe-COF_{TAPB-PDA} evaluated from TEM measurement and comparable to calculated values.

S5.4 Solid-state ^{13}C NMR, FTIR, and XPS spectra

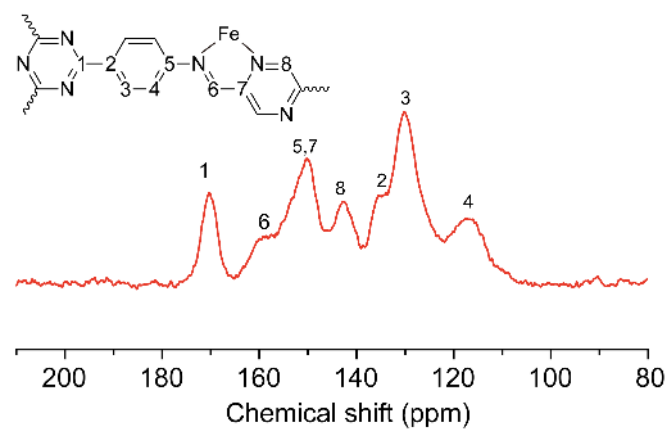


Fig. S37 Solid-state ^{13}C NMR spectra of Fe-COF_{TTA-PDA}.

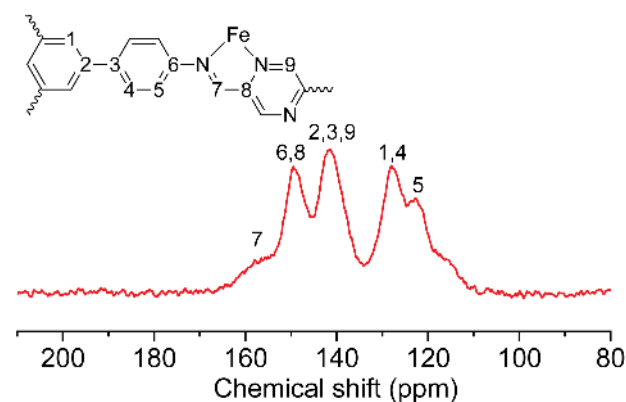


Fig. S38 Solid-state ^{13}C NMR spectra of Fe-COF_{TAPB-PDA}.

The emerging shoulder peaks around 159.3 ppm in solid-state NMR spectra can be indexed as the formation of imine bonds in Fe-iminopyrazine linkages.

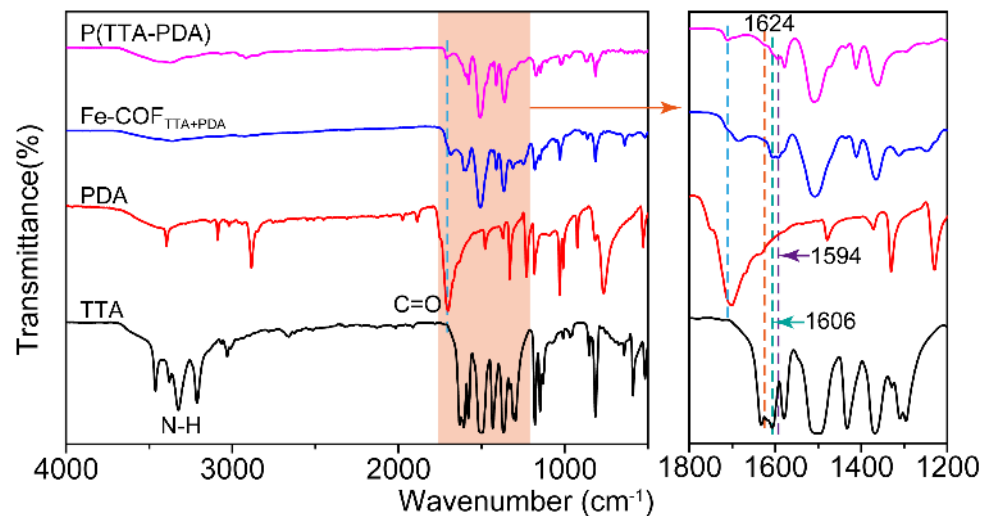


Fig. S39 FTIR spectra of Fe-COF_{TTA+PDA} compared to amorphous P(TTA-PDA), PDA, and TTA.

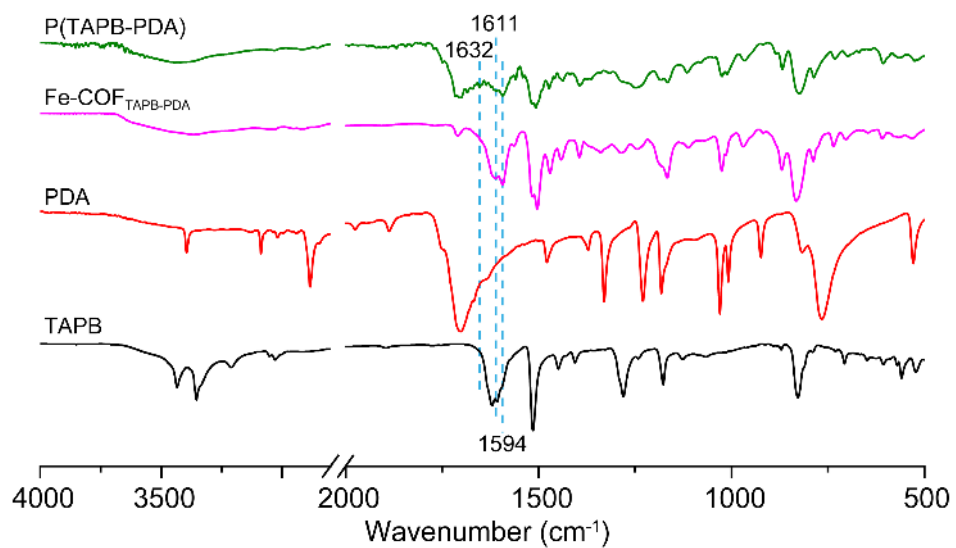


Fig. S40 FTIR spectra of Fe-COF_{TAPB-PDA} compared to amorphous P(TAPB-PDA), PDA, and TAPB.

Table S8. Typical FTIR peaks of imine bond in iminopyrazine-based Fe-COFs compared to amorphous powders without Fe(II).

Entry	P(TTA-PDA)	Fe-COF _{TTA-PDA}	P(TAPB-PDA)	Fe-COF _{TAPB-PDA}
Imine bond				
	1624 cm ⁻¹	1606 cm ⁻¹	1632 cm ⁻¹	1611 cm ⁻¹
vibration mode				

FTIR spectra not only indicate the consumption of monomers and the formation of imine bonds but also demonstrate the Fe coordination via the vibration peak shift (Table S8), which is further confirmed by XPS spectra.

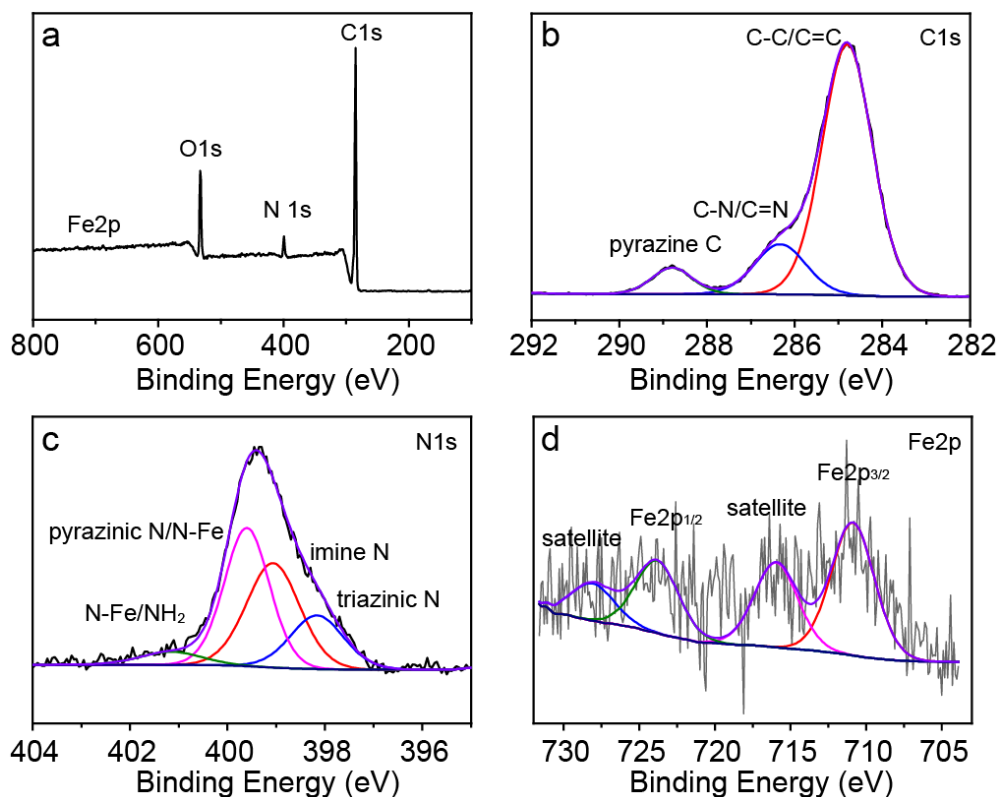


Fig. S41 XPS spectra of Fe-COF_{TTA-PDA}. (a) Survey spectrum, (b) C1s, (c) N1s, and (d) Fe2p cores.

S6. Atomic parameters of refined Fe-COF models and calculated parameters.

Table S9. Atomic parameters of Eclipsed Fe-COF_{TTA-BPA} with *P*1 space group.

No.	Atom	x	y	z	No	Atom	x	y	z
1	C1	0.47218	0.56328	0.64762	41	H41	0.48794	0.91584	1.00165
2	C2	0.45596	0.52949	0.79684	42	H42	0.51457	0.97955	1.019
3	C3	0.47327	0.51016	0.76923	43	H43	0.42186	0.96915	0.43785
4	C4	0.50663	0.52391	0.58168	44	H44	0.44098	0.8588	0.75908
5	C5	0.52167	0.55877	0.43647	45	H45	0.33229	0.79497	0.68487
6	N6	0.5052	0.57816	0.49122	46	H46	0.31195	0.7335	0.56918
7	C7	0.45139	0.58051	0.58739	47	H47	0.41643	0.76269	0.12478
8	N8	0.46493	0.6092	0.3885	48	H48	0.43506	0.8244	0.21949
9	C9	0.44208	0.62403	0.30316	49	C49	0.09851	0.54078	0.49615
10	C10	0.45155	0.65829	0.41379	50	C50	0.0783	0.55682	0.57753
11	C11	0.42768	0.67107	0.37575	51	C51	0.04152	0.53835	0.51067
12	C12	0.39244	0.64887	0.24973	52	C52	0.02511	0.50437	0.35612
13	C13	0.38202	0.61405	0.15507	53	C53	0.04771	0.49117	0.2412
14	C14	0.40621	0.60179	0.18654	54	N54	0.08364	0.50962	0.3153
15	C15	0.64778	0.34824	0.76539	55	C55	0.13623	0.55708	0.59691
16	N16	0.63162	0.31272	0.77792	56	N56	0.15479	0.54233	0.49383
17	H17	0.42947	0.51772	0.92246	57	C57	0.19281	0.56687	0.40699
18	H18	0.45947	0.48447	0.89454	58	C58	0.22071	0.56213	0.54349
19	H19	0.54443	0.56935	0.25276	59	C59	0.25683	0.58675	0.48158
20	H20	0.42392	0.5673	0.68074	60	C60	0.26671	0.61926	0.31548
21	H21	0.47642	0.67457	0.55415	61	C61	0.23964	0.62613	0.20306
22	H22	0.43595	0.69756	0.46921	62	C62	0.20349	0.60037	0.24491
23	H23	0.35473	0.59595	0.06657	63	C63	0.70408	0.35164	0.77589
24	H24	0.39597	0.5741	0.14103	64	N64	0.68412	0.36768	0.76415
25	C25	0.43847	0.90715	0.74716	65	H65	0.09043	0.58223	0.71554
26	C26	0.47283	0.92773	0.89638	66	H66	0.02591	0.54954	0.6112
27	C27	0.48822	0.96392	0.89796	67	H67	0.03639	0.46591	0.10744
28	C28	0.46974	0.97977	0.74633	68	H68	0.14888	0.58396	0.69292
29	C29	0.43484	0.95767	0.59491	69	H69	0.21579	0.54078	0.71976
30	N30	0.41934	0.92175	0.61328	70	H70	0.27723	0.58146	0.59043
31	C31	0.42485	0.87012	0.67544	71	H71	0.24651	0.65138	0.08077
32	N32	0.39516	0.85226	0.48844	72	H72	0.18391	0.60762	0.16567
33	C33	0.38302	0.81549	0.40534	73	C73	0.55253	0.45768	0.38035
34	C34	0.34947	0.7887	0.52816	74	C74	0.57111	0.49254	0.25687
35	C35	0.33841	0.75323	0.47321	75	C75	0.55691	0.51436	0.32981
36	C36	0.36215	0.74323	0.32304	76	C76	0.52375	0.50136	0.51798
37	C37	0.39708	0.7696	0.22958	77	C77	0.50752	0.46612	0.64968
38	C38	0.40741	0.80512	0.27356	78	N78	0.52289	0.44597	0.59296
39	C39	0.65126	0.29645	0.79011	79	C79	0.56582	0.43367	0.31777
40	N40	0.68753	0.31605	0.78823	80	N80	0.55339	0.40528	0.52476

81	C81	0.57873	0.39305	0.62636	124	C124	0.98521	0.48112	0.37236
82	C82	0.56801	0.36193	0.82718	125	C125	0.96098	0.49421	0.36273
83	C83	0.58995	0.34715	0.86794	126	N126	0.9251	0.47243	0.42111
84	C84	0.62548	0.36513	0.74173	127	C127	0.87709	0.41994	0.69906
85	C85	0.63898	0.39901	0.59376	128	N128	0.85795	0.43522	0.70434
86	C86	0.61615	0.41282	0.53766	129	C129	0.81938	0.41345	0.73058
87	C87	0.36557	0.66058	0.25107	130	C130	0.79957	0.42559	0.91927
88	N88	0.37588	0.69522	0.26592	131	C131	0.762	0.40657	0.92278
89	H89	0.596	0.50252	0.10072	132	C132	0.74367	0.37266	0.76544
90	H90	0.57157	0.54065	0.2225	133	C133	0.76364	0.3586	0.60429
91	H91	0.4835	0.45491	0.80132	134	C134	0.80099	0.37907	0.57807
92	H92	0.58887	0.44275	0.13558	135	C135	0.30508	0.64621	0.28092
93	H93	0.5434	0.34921	0.96928	136	N136	0.33017	0.63631	0.26102
94	H94	0.57946	0.32205	1.01106	137	H137	0.92517	0.39755	0.63788
95	H95	0.66685	0.41423	0.50779	138	H138	0.98846	0.43452	0.49303
96	H96	0.6287	0.43916	0.42597	139	H139	0.97091	0.52159	0.34446
97	C97	0.52596	0.09055	0.90873	140	H140	0.86639	0.39295	0.79117
98	C98	0.48952	0.07137	0.9961	141	H141	0.8143	0.44795	1.0949
99	C99	0.47083	0.03541	0.93141	142	H142	0.74736	0.4171	1.07077
100	C100	0.4877	0.01889	0.75829	143	H143	0.75014	0.33247	0.48147
101	C101	0.52414	0.03999	0.65331	144	H144	0.81532	0.36836	0.42849
102	N102	0.54321	0.07486	0.75015	145	O145	0.46685	0.3802	0.46295
103	C103	0.54611	0.12843	0.96531	146	S146	0.42726	0.36826	0.7304
104	N104	0.57925	0.14538	0.85481	147	C147	0.41592	0.39987	0.9573
105	C105	0.59794	0.18326	0.8255	148	O148	0.39348	0.34236	0.5061
106	C106	0.63279	0.20365	0.96437	149	O149	0.4258	0.33969	0.98717
107	C107	0.65073	0.2404	0.94336	150	F150	0.38326	0.38227	1.14011
108	C108	0.63308	0.25759	0.80063	151	F151	0.4121	0.42217	0.71358
109	C109	0.5975	0.23726	0.67398	152	F152	0.44329	0.42049	1.19777
110	C110	0.5803	0.20057	0.68251	153	O153	0.49295	0.35108	1.01295
111	C111	0.35096	0.70551	0.28635	154	S154	0.47426	0.31147	0.74443
112	N112	0.3156	0.68085	0.29354	155	C155	0.45424	0.26559	0.92741
113	H113	0.47617	0.08393	1.12977	156	O156	0.50474	0.31709	0.4768
114	H114	0.44441	0.02065	1.0458	157	O157	0.44679	0.31273	0.47998
115	H115	0.53675	0.02754	0.51336	158	F158	0.44274	0.23967	0.66033
116	H116	0.53264	0.14197	1.07166	159	F159	0.42367	0.25759	1.12953
117	H117	0.64524	0.19102	1.10641	160	F160	0.47994	0.26231	1.12737
118	H118	0.67775	0.25546	1.05484	161	Fe161	0.50749	0.39801	0.80773
119	H119	0.58328	0.24983	0.56109	162	O162	0.56216	0.62872	0.0152
120	H120	0.55315	0.18561	0.57661	163	S163	0.60017	0.64496	0.31772
121	C121	0.913	0.43903	0.54202	164	C164	0.61648	0.61616	0.51956
122	C122	0.93514	0.42435	0.54419	165	O165	0.6329	0.67119	0.08365
123	C123	0.97114	0.44541	0.45679	166	O166	0.60028	0.67392	0.5598

167	F167	0.64839	0.63595	0.70992	207	O207	0.21145	0.50132	0.26079
168	F168	0.62461	0.59792	0.26167	208	O208	0.16357	0.49958	-0.03665
169	F169	0.58971	0.59134	0.74175	209	F209	0.17435	0.41029	-0.00589
170	O170	0.53594	0.65712	0.57055	210	F210	0.14347	0.41403	0.45475
171	S171	0.54746	0.6967	0.33467	211	F211	0.20469	0.44377	0.46265
172	C172	0.55819	0.7408	0.51723	212	Fe212	0.1179	0.49142	0.30441
173	O173	0.51635	0.68424	0.05514	213	O213	0.91517	0.53057	0.22301
174	O174	0.57815	0.70179	0.07147	214	S214	0.93836	0.56951	0.48772
175	F175	0.56457	0.76581	0.25051	215	C215	0.98376	0.58637	0.68568
176	F176	0.58975	0.75469	0.72002	216	O216	0.94196	0.60073	0.25387
177	F177	0.52922	0.73764	0.71795	217	O217	0.90875	0.56779	0.73501
178	Fe178	0.51485	0.62109	0.19305	218	F218	0.99457	0.61729	0.87999
179	O179	0.36247	0.91987	0.14648	219	F219	1.01052	0.59467	0.42641
180	S180	0.33988	0.93539	0.44315	220	F220	0.98236	0.56016	0.90119
181	C181	0.36358	0.98028	0.64914	221	O221	0.84947	0.49631	0.69202
182	O182	0.3099	0.93588	0.20945	222	S222	0.83101	0.51877	0.44933
183	O183	0.3139	0.90445	0.6893	223	C223	0.81133	0.54537	0.63341
184	F184	0.34006	0.98786	0.83486	224	O224	0.80237	0.49064	0.19056
185	F185	0.38118	1.00753	0.39842	225	O225	0.8605	0.54197	0.17621
186	F186	0.38919	0.98112	0.87962	226	F226	0.80004	0.56018	0.36597
187	O187	0.34003	0.86536	0.69493	227	F227	0.83715	0.57382	0.83276
188	S188	0.30064	0.83389	0.46172	228	F228	0.78063	0.52366	0.83469
189	C189	0.25762	0.7966	0.64312	229	Fe229	0.88677	0.48569	0.50407
190	O190	0.31624	0.81888	0.17955	230	O230	0.645	0.15291	0.60238
191	O191	0.29144	0.8561	0.19835	231	S231	0.67692	0.14799	0.34028
192	F192	0.23321	0.77585	0.37594	232	C232	0.71569	0.18723	0.12486
193	F193	0.24005	0.8103	0.84605	233	O233	0.69036	0.12589	0.55174
194	F194	0.26458	0.77367	0.84282	234	O234	0.65259	0.11969	0.06505
195	Fe195	0.37669	0.88521	0.31355	235	F235	0.73603	0.17665	-0.07776
196	O196	0.08158	0.44772	0.08137	236	F236	0.73909	0.21155	0.37892
197	S197	0.05717	0.41412	0.4036	237	F237	0.70307	0.20477	-0.09182
198	C198	0.00987	0.38287	0.21986	238	O238	0.61003	0.07823	0.49443
199	O199	0.06269	0.38784	0.17101	239	S239	0.60541	0.04206	0.75834
200	O200	0.08756	0.41153	0.59628	240	C240	0.59893	-0.00053	0.57457
201	F201	0.0046	0.35348	0.01314	241	O241	0.5752	0.03439	1.0344
202	F202	0.00199	0.40417	0.00502	242	O242	0.63929	0.05804	1.00897
203	F203	-0.01709	0.36901	0.48133	243	F243	0.59553	-0.02459	0.84093
204	O204	0.14801	0.46901	0.3671	244	F244	0.62901	0.00603	0.37142
205	S205	0.17916	0.47521	0.02223	245	F245	0.56724	-0.0174	0.37426
206	C206	0.17421	0.43381	0.24818	246	Fe246	0.59587	0.11203	0.67565

Table S10. Simulated topological models for Fe-COF_{TTA-BPA} with corresponding cell

parameters and porous properties.

Topological Models	Cell parameters ($\alpha = \beta = 90^\circ$, $\gamma = 120^\circ$)	Free volume per cell (\AA^2)	Surface area per cell (\AA^3)	Surface area (m^2/g)	Pore volume (cm^3/g)	Pore size (nm)
Fe-COF_{TTA-BPA} (P1_AA_6Fe)	$a = 43.0198\text{\AA}$ $b = 43.9075\text{\AA}$ $c = 3.5249\text{\AA}$	2876.23	505.29	905.31	0.592	3.06
P1_AA_3Fe-1	$a = 43.8597\text{\AA}$ $b = 43.5508\text{\AA}$ $c = 3.5255\text{\AA}$	2921.62	530.22	1388.72	0.765	3.44
P1_AA_3Fe-2	$a = 43.9131\text{\AA}$ $b = 43.1364\text{\AA}$ $c = 3.7455\text{\AA}$	3062.20	564.48	1478.45	0.802	3.32
COF_{TTA-BPA} AA without Fe	$a = b = 43.8108\text{\AA}$ $c = 3.4655\text{\AA}$	3483.47	466.11	2268.51	1.695	3.78
COF_{TTA-BPA} AB without Fe	$a = b = 43.8049\text{\AA}$ $c = 5.9681\text{\AA}$	3546.99	1599.62	3892.59	0.863	-

Table S11. Atomic parameters of Eclipsed Fe-COF_{TAPB-BPA} with *P1* space group.

No.	Atom	x	y	z	No.	Atom	x	y	z
1	C1	0.4913	0.57498	0.66997	41	H41	0.47047	0.91383	1.11869
2	C2	0.49235	0.55182	0.83543	42	H42	0.49573	0.9787	1.10963
3	C3	0.51355	0.5366	0.78882	43	H43	0.44443	0.96781	0.43546
4	C4	0.532	0.54293	0.57228	44	H44	0.4328	0.85301	0.90748
5	C5	0.53194	0.5685	0.41785	45	H45	0.35709	0.79762	0.8352
6	N6	0.51284	0.58486	0.47603	46	H46	0.3318	0.73366	0.75769
7	C7	0.46395	0.58577	0.67817	47	H47	0.40511	0.75927	0.16941
8	N8	0.46195	0.60265	0.49509	48	H48	0.42973	0.82312	0.25037
9	C9	0.436	0.61406	0.47331	49	C49	0.08885	0.54773	0.35198
10	C10	0.43327	0.6352	0.64906	50	C50	0.06514	0.55951	0.41403
11	C11	0.4096	0.64829	0.62204	51	C51	0.0283	0.53529	0.41878
12	C12	0.38758	0.63957	0.42026	52	C52	0.01471	0.49943	0.3547
13	C13	0.38974	0.61759	0.24673	53	C53	0.04	0.48984	0.27396
14	C14	0.41425	0.60537	0.27199	54	N54	0.07593	0.51394	0.2781
15	C15	0.65105	0.35015	0.76349	55	C55	0.12811	0.56989	0.37707
16	C16	0.62905	0.31416	0.81634	56	N56	0.14752	0.55504	0.33949
17	H17	0.47591	0.54465	0.99373	57	C57	0.18627	0.57553	0.32282
18	H18	0.51454	0.51897	0.91895	58	C58	0.20794	0.56497	0.44256
19	H19	0.54491	0.57354	0.24746	59	C59	0.24551	0.58655	0.44547
20	H20	0.44487	0.57777	0.82174	60	C60	0.2623	0.61954	0.32808
21	H21	0.45028	0.6422	0.80362	61	C61	0.24058	0.62959	0.20028
22	H22	0.40839	0.66523	0.75844	62	C62	0.20303	0.60785	0.19842
23	H23	0.37299	0.61056	0.09028	63	C63	0.7039	0.34386	0.81037
24	H24	0.41595	0.58873	0.13693	64	C64	0.6885	0.36489	0.76165
25	C25	0.44037	0.90512	0.7938	65	H65	0.07519	0.58657	0.47303
26	C26	0.46382	0.92587	0.97429	66	H66	0.01111	0.54481	0.48406
27	C27	0.47862	0.96255	0.96592	67	H67	0.03142	0.4632	0.21683
28	C28	0.47114	0.9782	0.77338	68	H68	0.14019	0.5977	0.42228
29	C29	0.44839	0.95619	0.59247	69	H69	0.19571	0.5403	0.53791
30	N30	0.43188	0.92029	0.61416	70	H70	0.26128	0.5781	0.54711
31	C31	0.42654	0.86704	0.77556	71	H71	0.25257	0.65442	0.10434
32	N32	0.40832	0.85147	0.58664	72	H72	0.18686	0.61626	0.10134
33	C33	0.39445	0.81451	0.54435	73	C73	0.5808	0.48048	0.39973
34	C34	0.36726	0.78914	0.6895	74	C74	0.5964	0.51498	0.31254
35	C35	0.35292	0.75298	0.64413	75	C75	0.58	0.53509	0.36301
36	C36	0.36642	0.7418	0.45633	76	C76	0.54896	0.52126	0.5065
37	C37	0.39424	0.76739	0.31418	77	C77	0.53409	0.48593	0.58632
38	C38	0.40799	0.80357	0.35762	78	N78	0.54998	0.46674	0.52694
39	C39	0.64416	0.29274	0.86177	79	C79	0.59771	0.45851	0.38145
40	C40	0.68171	0.30786	0.86087	80	N80	0.58121	0.42771	0.48565

81	C81	0.59976	0.40925	0.55553	124	C124	0.98312	0.47203	0.39633
82	C82	0.59271	0.39276	0.77699	125	C125	0.95675	0.48194	0.43733
83	C83	0.60905	0.37321	0.84429	126	N126	0.92303	0.45738	0.50954
84	C84	0.63457	0.37172	0.69607	127	C127	0.87495	0.39876	0.60628
85	C85	0.64304	0.38967	0.47846	128	N128	0.85585	0.41347	0.65956
86	C86	0.62564	0.40815	0.4085	129	C129	0.81805	0.39345	0.71058
87	C87	0.36276	0.65374	0.39281	130	C130	0.8042	0.40122	0.91196
88	C88	0.37583	0.69007	0.42025	131	C131	0.76695	0.38454	0.94878
89	H89	0.62108	0.52625	0.21006	132	C132	0.7432	0.35906	0.7867
90	H90	0.59228	0.56165	0.29454	133	C133	0.75715	0.34974	0.59272
91	H91	0.50963	0.47334	0.69013	134	C134	0.79437	0.36703	0.55405
92	H92	0.62496	0.46985	0.31432	135	C135	0.30192	0.64403	0.34905
93	H93	0.57475	0.3954	0.8986	136	C136	0.32595	0.63092	0.35232
94	H94	0.60208	0.35938	1.01258	137	H137	0.92836	0.38296	0.49845
95	H95	0.66231	0.38847	0.36006	138	H138	0.9907	0.42594	0.39948
96	H96	0.63215	0.42134	0.23873	139	H139	0.96295	0.50896	0.41646
97	C97	0.51091	0.08437	0.80639	140	H140	0.86376	0.37033	0.61357
98	C98	0.47446	0.06163	0.75538	141	H141	0.82254	0.4205	1.03763
99	C99	0.46183	0.02537	0.73442	142	H142	0.75655	0.39175	1.1007
100	C100	0.48533	0.01206	0.76883	143	H143	0.7391	0.33023	0.46613
101	C101	0.52198	0.0361	0.81321	144	H144	0.80481	0.3606	0.39873
102	N102	0.533362	0.07135	0.82871	145	O145	0.51012	0.40411	0.30478
103	C103	0.52645	0.12272	0.84159	146	S146	0.4676	0.3992	0.34102
104	N104	0.56066	0.1411	0.89117	147	C147	0.45904	0.43476	0.25159
105	C105	0.58008	0.17918	0.89401	148	O148	0.44181	0.3646	0.20688
106	C106	0.60473	0.19786	1.07498	149	O149	0.457	0.38776	0.6021
107	C107	0.6254	0.23496	1.0685	150	F150	0.43009	0.42149	0.0975
108	C108	0.62076	0.25387	0.88306	151	F151	0.48916	0.46115	0.13973
109	C109	0.59498	0.23515	0.70721	152	F152	0.45127	0.44856	0.44886
110	C110	0.57504	0.19819	0.71157	153	O153	0.51654	0.36772	0.69716
111	C111	0.35235	0.70355	0.41525	154	S154	0.51178	0.33937	0.46351
112	C112	0.31545	0.68048	0.38169	155	C155	0.51547	0.3001	0.52615
113	H113	0.45616	0.07175	0.73471	156	O156	0.5365	0.36172	0.25771
114	H114	0.43347	0.0075	0.70065	157	O157	0.47396	0.32742	0.36038
115	H115	0.54065	0.02645	0.83583	158	F158	0.50332	0.27755	0.33332
116	H116	0.51006	0.13517	0.82168	159	F159	0.49493	0.28287	0.72217
117	H117	0.60801	0.18351	1.21966	160	F160	0.55101	0.31013	0.56938
118	H118	0.64503	0.24894	1.20615	161	Fe161	0.53257	0.41674	0.61107
119	H119	0.59143	0.24919	0.56092	162	O162	0.54211	0.62751	0.04821
120	H120	0.55633	0.18425	0.56903	163	S163	0.58714	0.65275	0.14476
121	C121	0.91233	0.4225	0.52925	164	C164	0.61794	0.63519	0.14505
122	C122	0.93655	0.41073	0.48127	165	O165	0.60311	0.68343	-0.03758
123	C123	0.97201	0.43555	0.4198	166	O166	0.59085	0.67405	0.37263

167	F167	0.6524	0.66194	0.08943	210	F210	0.13193	0.4279	-0.13548
168	F168	0.60688	0.60828	-0.0198	211	F211	0.18839	0.44747	-0.00355
169	F169	0.61842	0.62264	0.36929	212	Fe212	0.11608	0.50375	0.25473
170	O170	0.5289	0.65715	0.46112	213	O213	0.91391	0.51646	0.58601
171	S171	0.52432	0.69069	0.32922	214	S214	0.93139	0.53326	0.86302
172	C172	0.52613	0.72609	0.51256	215	C215	0.97976	0.5535	0.91954
173	O173	0.49015	0.67222	0.17351	216	O216	0.91891	0.56052	0.91196
174	O174	0.55401	0.70642	0.13795	217	O217	0.90842	0.5038	1.04438
175	F175	0.52377	0.75064	0.37023	218	F218	0.98769	0.56957	1.13954
176	F176	0.55837	0.74254	0.6351	219	F219	0.99867	0.57862	0.74764
177	F177	0.49791	0.71216	0.67144	220	F220	0.98936	0.52755	0.91552
178	Fe178	0.50245	0.61592	0.26872	221	O221	0.84631	0.47289	0.74394
179	O179	0.39286	0.9164	0.17749	222	S222	0.8257	0.47973	0.50291
180	S180	0.37311	0.93885	0.31193	223	C223	0.82004	0.51861	0.50307
181	C181	0.38762	0.98434	0.21869	224	O224	0.78898	0.44509	0.47926
182	O182	0.33241	0.91615	0.25697	225	O225	0.84601	0.47774	0.28286
183	O183	0.37317	0.93478	0.58398	226	F226	0.80249	0.51901	0.29845
184	F184	0.37152	0.99829	0.36108	227	F227	0.85355	0.54895	0.51258
185	F185	0.37744	0.98411	-0.01352	228	F228	0.80001	0.51739	0.69836
186	F186	0.42463	1.00515	0.23625	229	Fe229	0.88447	0.46618	0.62444
187	O187	0.35573	0.86915	0.54733	230	O230	0.62992	0.14902	0.97174
188	S188	0.32209	0.83306	0.39308	231	S231	0.65194	0.16233	0.70276
189	C189	0.28164	0.80012	0.54892	232	C232	0.68279	0.20934	0.64449
190	O190	0.34085	0.8161	0.2558	233	O233	0.6717	0.14088	0.67946
191	O191	0.31141	0.8491	0.18544	234	O234	0.6223	0.14457	0.51237
192	F192	0.25803	0.77535	0.38866	235	F235	0.70364	0.21293	0.4486
193	F193	0.26516	0.8168	0.65592	236	F236	0.70492	0.22458	0.83809
194	F194	0.29095	0.78333	0.71878	237	F237	0.66329	0.22617	0.60139
195	Fe195	0.39975	0.88364	0.37751	238	O238	0.60254	0.07902	0.89508
196	O196	0.08457	0.45571	0.15534	239	S239	0.60188	0.06575	1.18449
197	S197	0.07399	0.42902	0.40312	240	C240	0.59713	0.0223	1.2424
198	C198	0.02982	0.38856	0.41447	241	O241	0.57384	0.07201	1.3162
199	O199	0.10492	0.42053	0.42084	242	O242	0.63767	0.09526	1.29031
200	O200	0.08159	0.45367	0.61821	243	F243	0.5959	0.0166	1.48427
201	F201	0.03414	0.35919	0.41535	244	F244	0.62613	0.02097	1.14738
202	F202	0.00978	0.38724	0.21905	245	F245	0.56576	-0.00387	1.14092
203	F203	0.01197	0.38869	0.61827	246	Fe246	0.58303	0.11026	0.89992
204	O204	0.15537	0.49465	0.25899	247	H247	0.60002	0.30247	0.81356
205	S205	0.16835	0.49552	-0.02994	248	H248	0.69364	0.29134	0.89016
206	C206	0.16699	0.4556	-0.14326	249	H249	0.7057	0.39264	0.71716
207	O207	0.20686	0.5281	-0.0413	250	H250	0.40436	0.70789	0.45076
208	O208	0.14613	0.50801	-0.17541	251	H251	0.29723	0.69095	0.38598
209	F209	0.17971	0.46123	-0.37264	252	H252	0.31598	0.6028	0.32964

Table S12. Simulated topological models for Fe-COF_{TAPB-BPA} with corresponding cell parameters and porous properties.

Topological Models	Fe-COF _{TAPB-BPA}	COF _{TAPB-BPA AA} without Fe	COF _{TAPB-BPA AB} without Fe
Cell parameters $(\alpha = \beta = 90^\circ, \gamma = 120^\circ)$	$a = 42.8224 \text{ \AA}$ $b = 43.5567 \text{ \AA}$ $c = 5.6515 \text{ \AA}$	$a = b = 45.2386 \text{ \AA}$ $c = 3.4699 \text{ \AA}$	$a = b = 43.8049 \text{ \AA}$ $c = 6.2876 \text{ \AA}$
Free volume per cell (\AA^3)	4331.64	3796.11	4308.70
Surface area per cell (\AA^2)	892.08	485.79	1795.41
Surface area (m^2/g)	1601.13	2375.67	4390.05
Pore volume (cm^3/g)	0.777	1.865	1.053
Pore size (nm)	3.12	3.82	-

Table S13. Atomic parameters of Eclipsed Fe-COF_{TTA-PDA} with *P1* space group.

No.	Atom	x	y	z	No	Atom	x	y	z
1	N1	0.29577	0.69223	0.65637	41	N41	0.36145	0.69976	0.63416
2	C2	0.27844	0.64949	0.61455	42	C42	0.36986	0.63688	0.56111
3	C3	0.33725	0.78549	0.57217	43	C43	0.33723	0.71749	0.66708
4	C4	0.35574	0.76453	0.69631	44	C44	0.40171	0.65198	0.37187
5	C5	0.39222	0.78905	0.84119	45	C45	0.36139	0.60095	0.71641
6	C6	0.40992	0.83391	0.85825	46	C46	0.3845	0.58053	0.68376
7	C7	0.39245	0.85539	0.72256	47	C47	0.41587	0.5951	0.49187
8	C8	0.35568	0.83018	0.58256	48	C48	0.42435	0.63078	0.33808
9	N9	0.43895	0.5734	0.45477	49	C49	0.08125	0.5642	0.48214
10	C10	0.42103	0.53167	0.46198	50	C50	0.03636	0.53698	0.45952
11	C11	0.44709	0.5132	0.51971	51	C51	0.00934	0.55332	0.4473
12	C12	0.4326	0.46888	0.51675	52	H52	0.40852	0.67957	0.24951
13	N13	0.45984	0.45474	0.55476	53	H53	0.33717	0.58908	0.86476
14	H14	0.30899	0.76728	0.4602	54	H54	0.37835	0.5535	0.80967
15	H15	0.40669	0.7733	0.94183	55	H55	0.44853	0.64154	0.19259
16	H16	0.43746	0.85189	0.97626	56	H56	0.09529	0.5989	0.49597
17	H17	0.3407	0.8447	0.48162	57	H57	0.02149	0.58731	0.41831
18	H18	0.3878	0.51142	0.45068	58	N58	0.51354	0.42475	0.54245
19	H19	0.40073	0.44673	0.47296	59	N59	0.48719	0.54131	0.57413
20	N20	0.41325	0.90217	0.71403	60	N60	0.67621	0.32485	0.49419
21	N21	0.53056	0.03112	0.64056	61	C61	0.69172	0.36779	0.47573
22	N22	0.30277	0.63205	0.58247	62	C62	0.63106	0.23186	0.68469
23	C23	0.34417	0.65697	0.5925	63	C63	0.61809	0.25094	0.49315
24	C24	0.21671	0.59127	0.38724	64	C64	0.58839	0.2248	0.30512
25	C25	0.23335	0.6222	0.58952	65	C65	0.57215	0.18025	0.3084
26	C26	0.20657	0.62702	0.76294	66	C66	0.58431	0.16096	0.5041
27	C27	0.16381	0.6007	0.73559	67	C67	0.61367	0.18707	0.69214
28	C28	0.14711	0.56997	0.53141	68	C68	0.52835	0.46534	0.60286
29	C29	0.17407	0.56599	0.35621	69	C69	0.50017	0.48269	0.60479
30	C30	0.45348	0.92542	0.71619	70	C70	0.51415	0.52702	0.62379
31	C31	0.47254	0.97232	0.69396	71	H71	0.65388	0.25167	0.83144
32	C32	0.51535	1.00027	0.69409	72	H72	0.57835	0.23914	0.15419
33	H33	0.23684	0.58734	0.24974	73	H73	0.54951	0.16042	0.16121
34	H34	0.21883	0.65064	0.92158	74	H74	0.62192	0.17227	0.84794
35	H35	0.14343	0.60407	0.87338	75	H75	0.56075	0.48668	0.64312
36	H36	0.16251	0.54359	0.19523	76	H76	0.54612	0.5493	0.66394
37	H37	0.4729	0.91105	0.71862	77	N77	0.44688	0.98845	0.66628
38	H38	0.5357	0.98796	0.7333	78	N78	0.56368	0.11494	0.52799
39	N39	0.10306	0.54514	0.49556	79	N79	0.66592	0.38384	0.46061
40	N40	0.94888	0.52546	0.46258	80	C80	0.73664	0.3968	0.46985

81	C81	0.62464	0.35703	0.46663	124	S124	0.51857	0.67094	0.88584
82	C82	0.82298	0.44944	0.44475	125	O125	0.52999	0.67881	1.18316
83	C83	0.50471	0.04674	0.59894	126	O126	0.56207	0.68963	0.76517
84	C84	0.755	0.4274	0.26652	127	C127	0.49643	0.70428	0.78534
85	C85	0.76167	0.39277	0.66128	128	F128	0.45576	0.68569	0.86258
86	C86	0.80442	0.41931	0.65081	129	F129	0.49906	0.70973	0.51347
87	C87	0.79793	0.45271	0.25164	130	F130	0.51856	0.74422	0.90403
88	C88	0.52365	0.09251	0.53658	131	S131	0.58096	0.62126	0.25505
89	C89	0.46193	0.0195	0.62097	132	C132	0.62374	0.67081	0.11931
90	H90	0.73615	0.43043	0.11448	133	F133	0.62833	0.66552	-0.14746
91	H91	0.74805	0.36908	0.81873	134	O134	0.54543	0.59489	0.05973
92	H92	0.82343	0.41623	0.80143	135	O135	0.59638	0.58929	0.31285
93	H93	0.81192	0.47404	0.08664	136	F136	0.61607	0.7043	0.15404
94	H94	0.50466	0.10718	0.5109	137	F137	0.65968	0.68035	0.25064
95	H95	0.44168	0.03253	0.60414	138	S138	0.36722	0.36276	0.21863
96	N96	0.02115	0.49393	0.457	139	O139	0.33884	0.38244	0.24541
97	N97	0.86712	0.47355	0.42142	140	O140	0.39969	0.3948	0.02222
98	C98	0.6351	0.29788	0.48909	141	C141	0.33557	0.30764	0.09504
99	C99	0.5411	0.40707	0.51832	142	F142	0.34029	0.27958	0.25953
100	C100	0.93375	0.48227	0.46371	143	F143	0.29459	0.2967	0.09332
101	N101	0.60945	0.31402	0.47654	144	F144	0.34744	0.30448	-0.15933
102	C102	0.55616	0.34885	0.57994	145	S145	0.45435	0.33341	0.18338
103	C103	0.59605	0.37431	0.47782	146	O146	0.41564	0.30078	0.02796
104	C104	0.60851	0.41648	0.39643	147	O147	0.47868	0.30923	0.20781
105	C105	0.58133	0.43248	0.41478	148	C148	0.48054	0.3857	0.03613
106	C106	0.52933	0.36511	0.60096	149	F149	0.47468	0.41723	0.14206
107	C107	0.88897	0.45478	0.44684	150	F150	0.52181	0.40038	0.00479
108	C108	0.96076	0.46584	0.46169	151	F151	0.46098	0.37781	-0.18561
109	H109	0.54586	0.31639	0.64886	152	S152	0.12531	0.47091	0.75031
110	H110	0.63905	0.43683	0.31573	153	O153	0.13596	0.4346	0.7793
111	H111	0.59134	0.46454	0.34095	154	O154	0.16733	0.51181	0.80026
112	H112	0.49955	0.34458	0.68694	155	C155	0.08392	0.4644	0.95503
113	H113	0.87472	0.42005	0.46052	156	F156	0.04862	0.45579	0.82494
114	H114	0.94868	0.43149	0.45894	157	F157	0.07559	0.42922	1.1013
115	Fe115	0.50034	0.60134	0.49551	158	F158	0.0959	0.50171	1.09171
116	O116	0.02518	0.41963	0.37063	159	S159	0.02881	0.37728	0.51643
117	O117	0.11359	0.47153	0.42834	160	O160	-0.01201	0.33966	0.40722
118	O118	0.43684	0.3353	0.48721	161	O161	0.01486	0.37261	0.80885
119	O119	0.38975	0.37154	0.52992	162	C162	0.06527	0.35805	0.44426
120	Fe120	0.44874	0.39496	0.51386	163	F163	0.07299	0.34248	0.67469
121	O121	0.49435	0.61493	0.85504	164	F164	0.04821	0.3252	0.25966
122	O122	0.55855	0.62388	0.54969	165	F165	0.10203	0.39043	0.34445
123	Fe123	0.06646	0.4806	0.44169	166	O166	0.36911	0.98341	0.76125

167	O167	0.33169	0.89479	0.72109	192	F192	0.83661	0.61265	0.89672
168	Fe168	0.38834	0.94181	0.70018	193	S193	0.95125	0.61721	0.73771
169	S169	0.32904	0.88221	1.04195	194	O194	0.91623	0.58231	0.90609
170	O170	0.2894	0.88071	1.14308	195	O195	0.98739	0.61106	0.82759
171	O171	0.31737	0.8344	1.05161	196	C196	0.96246	0.67156	0.8255
172	C172	0.376	0.9201	1.20548	197	F197	1.00054	0.69354	0.9477
173	F173	0.40386	0.95662	1.08023	198	F198	0.96304	0.69338	0.59863
174	F174	0.36202	0.93527	1.39087	199	F199	0.93267	0.66925	0.99713
175	F175	0.39668	0.89978	1.28417	200	O200	0.64492	0.12611	0.59974
176	S176	0.35214	1.00165	0.49438	201	O201	0.61113	0.04195	0.72366
177	O177	0.35674	1.04442	0.6	202	Fe202	0.58913	0.07839	0.61664
178	O178	0.38606	1.01894	0.27756	203	S203	0.61245	0.01074	0.46246
179	C179	0.29992	0.96879	0.36255	204	O204	0.65403	0.03856	0.32079
180	F180	0.27729	0.9891	0.40498	205	O205	0.62212	-0.02201	0.59686
181	F181	0.30173	0.96289	0.09333	206	C206	0.571	-0.01761	0.22352
182	F182	0.28077	0.92944	0.49015	207	F207	0.5565	0.00924	0.14596
183	O183	0.94071	0.59953	0.40896	208	F208	0.58629	-0.02872	0.0089
184	O184	0.85889	0.54731	0.2991	209	F209	0.53951	-0.05502	0.33062
185	Fe185	0.90339	0.53804	0.40695	210	S210	0.65864	0.1396	0.27002
186	S186	0.83335	0.55371	0.56531	211	O211	0.68425	0.11798	0.20401
187	O187	0.78731	0.52326	0.49882	212	O212	0.61959	0.11242	0.10141
188	O188	0.83909	0.5305	0.80389	213	C213	0.68996	0.19623	0.17511
189	C189	0.84102	0.60741	0.62996	214	F214	0.72412	0.21585	0.33788
190	F190	0.87985	0.63803	0.54613	215	F215	0.70267	0.19908	-0.08504
191	F191	0.8122	0.6125	0.48817	216	F216	0.66763	0.2169	0.20113

Table S14. Simulated topological models for Fe-COF_{TTA-PDA} with corresponding cell parameters and porous properties.

Topological Models	Fe-COF _{TTA-PDA}	COF _{TTA-PDA} P6/m_AA	COF _{TTA-PDA} P63/m_AB
Cell parameters $(\alpha = \beta = 90^\circ, \gamma = 120^\circ)$	$a = 37.4706 \text{ \AA}$ $b = 35.8836 \text{ \AA}$ $c = 4.0774 \text{ \AA}$	$a = b = 36.6106 \text{ \AA}$ $c = 3.5136 \text{ \AA}$	$a = b = 37.6218 \text{ \AA}$ $c = 6.0262 \text{ \AA}$
Free volume per cell (\AA^3)	1949.40	2237.82	1984.26
Surface area per cell (\AA^2)	737.02	366.41	1107.15
Surface area (m^2/g)	1416.72	2186.73	3303.72
Pore volume (cm^3/g)	0.375	1.336	0.592
Pore size (nm)	2.24	3.19	-

Table S15. Atomic parameters of Eclipsed Fe-COF_{TAPB-PDA} with *P*1 space group.

No.	Atom	x	y	z	No.	Atom	x	y	z
1	C1	0.2908	0.70456	0.64416	41	C41	0.3642	0.72276	0.66716
2	C2	0.27787	0.66117	0.7207	42	C42	0.38396	0.66574	0.82204
3	C3	0.31962	0.7878	0.27995	43	C43	0.33397	0.7355	0.60336
4	C4	0.34707	0.78065	0.47984	44	C44	0.42352	0.68536	0.65995
5	C5	0.38723	0.81693	0.55235	45	C45	0.37448	0.63083	1.03511
6	C6	0.39959	0.85831	0.4222	46	C46	0.40236	0.61468	1.06939
7	C7	0.37223	0.86574	0.22223	47	C47	0.44062	0.63252	0.89037
8	C8	0.33172	0.82952	0.15827	48	C48	0.45136	0.66871	0.69603
9	N9	0.46647	0.6119	0.88991	49	C49	0.07483	0.55896	0.59752
10	C10	0.44923	0.57051	0.96055	50	C50	0.02924	0.53198	0.54749
11	C11	0.47683	0.55254	1.01784	51	C51	0.00333	0.55067	0.49699
12	C12	0.45994	0.50693	1.02518	52	H52	0.43129	0.71111	0.48432
13	N13	0.48522	0.48903	0.97648	53	H53	0.34553	0.6159	1.17802
14	H14	0.28893	0.76098	0.20682	54	H54	0.39404	0.58834	1.24121
15	H15	0.40912	0.81383	0.71445	55	H55	0.47972	0.68143	0.55318
16	H16	0.43086	0.885	0.48072	56	H56	0.0885	0.59409	0.62581
17	H17	0.30871	0.83113	0.00602	57	H57	0.01803	0.5856	0.47858
18	H18	0.41507	0.54883	0.96916	58	N58	0.52961	0.45748	0.67779
19	H19	0.4267	0.48752	1.02335	59	N59	0.51926	0.58042	0.99565
20	N20	0.38713	0.90924	0.08204	60	C60	0.67126	0.32689	0.36803
21	N21	0.50629	0.02812	0.13805	61	C61	0.69235	0.3725	0.38962
22	C22	0.30828	0.64885	0.77484	62	C62	0.61935	0.23016	0.53525
23	C23	0.35175	0.67963	0.75812	63	C63	0.60487	0.25394	0.35544
24	C24	0.21695	0.59067	0.5215	64	C64	0.56883	0.23093	0.1575
25	C25	0.23197	0.62792	0.71959	65	C65	0.54925	0.18525	0.12943
26	C26	0.20256	0.6345	0.89582	66	C66	0.5639	0.16105	0.30887
27	C27	0.15907	0.60385	0.87655	67	C67	0.59778	0.18427	0.52011
28	C28	0.14345	0.56713	0.66678	68	C68	0.55052	0.4987	0.75681
29	C29	0.17324	0.56187	0.48772	69	C69	0.52712	0.51709	0.91422
30	C30	0.42716	0.93358	0.00613	70	C70	0.54469	0.56279	0.93988
31	C31	0.44624	0.98112	0.01831	71	H71	0.6457	0.24696	0.70356
32	C32	0.49035	1.00813	0.05847	72	H72	0.557	0.24843	0.01335
33	H33	0.23891	0.58571	0.37268	73	H73	0.5234	0.16892	-0.04251
34	H34	0.21335	0.66288	1.05303	74	H74	0.60582	0.16667	0.68564
35	H35	0.13722	0.60887	1.02399	75	H75	0.58452	0.5186	0.71915
36	H36	0.16288	0.53814	0.29862	76	H76	0.57725	0.58302	0.88092
37	H37	0.44794	0.91984	-0.01279	77	N77	0.41961	0.99732	0.06846
38	H38	0.51063	0.99416	0.0565	78	N78	0.54208	0.11344	0.28933
39	N39	0.09797	0.54024	0.6056	79	C79	0.66882	0.39362	0.43108
40	N40	0.95994	0.52403	0.44379	80	C80	0.73947	0.39828	0.37402

81	C81	0.62446	0.36958	0.44783	124	S124	0.56019	0.72166	1.29018
82	C82	0.82966	0.44909	0.35241	125	O125	0.57176	0.7292	1.6445
83	C83	0.48044	0.04516	0.16607	126	O126	0.60657	0.73837	1.18333
84	C84	0.75999	0.43557	0.17562	127	C127	0.54419	0.76377	1.22497
85	C85	0.76433	0.38556	0.55494	128	F128	0.50574	0.75247	1.36445
86	C86	0.80882	0.41117	0.54942	129	F129	0.54042	0.77024	0.90417
87	C87	0.80441	0.45903	0.1561	130	F130	0.57531	0.80343	1.35115
88	C88	0.50098	0.09188	0.24067	131	S131	0.6256	0.66526	0.63381
89	C89	0.43626	0.01788	0.14107	132	C132	0.6722	0.71685	0.49733
90	H90	0.74162	0.44498	0.02178	133	F133	0.67443	0.71935	0.16837
91	H91	0.74933	0.35705	0.71228	134	O134	0.59843	0.62797	0.39615
92	H92	0.82693	0.40201	0.7082	135	O135	0.64571	0.64278	0.83107
93	H93	0.81939	0.48368	-0.02299	136	F136	0.66934	0.7521	0.61406
94	H94	0.48186	0.10768	0.23987	137	F137	0.70928	0.71945	0.61118
95	H95	0.41657	0.03118	0.20371	138	S138	0.3736	0.41269	0.73788
96	N96	0.013	0.48808	0.51923	139	O139	0.35703	0.43697	0.95335
97	N97	0.87582	0.47422	0.33602	140	O140	0.4016	0.45001	0.50578
98	C98	0.62699	0.30245	0.37988	141	C141	0.32439	0.36848	0.5543
99	C99	0.55176	0.43445	0.59986	142	F142	0.29856	0.33925	0.78714
100	C100	0.94314	0.48018	0.42709	143	F143	0.30219	0.38642	0.40962
101	C101	0.60375	0.32394	0.41687	144	F144	0.33365	0.34619	0.32543
102	C102	0.564	0.37387	0.70896	145	S145	0.40885	0.33175	0.94842
103	C103	0.59951	0.39213	0.50006	146	O146	0.38457	0.33184	0.64524
104	C104	0.61133	0.43233	0.34697	147	O147	0.36721	0.29555	1.10351
105	C105	0.58737	0.45299	0.394	148	C148	0.43844	0.31018	0.73054
106	C106	0.54105	0.39548	0.76223	149	F149	0.46383	0.33922	0.4964
107	C107	0.89741	0.45395	0.36968	150	F150	0.4632	0.30204	0.94057
108	C108	0.9697	0.46191	0.45101	151	F151	0.40981	0.27113	0.58305
109	H109	0.55487	0.34362	0.83911	152	S152	0.13234	0.45054	0.67146
110	H110	0.6384	0.447	0.18319	153	O153	0.17032	0.45464	0.47305
111	H111	0.5964	0.48349	0.2703	154	O154	0.15923	0.48947	0.89825
112	H112	0.5158	0.38298	0.94108	155	C155	0.10992	0.39556	0.84549
113	H113	0.88223	0.41847	0.37204	156	F156	0.09922	0.36536	0.59895
114	H114	0.95646	0.42845	0.39183	157	F157	0.13978	0.39299	1.03716
115	Fe115	0.53124	0.64168	0.87548	158	F158	0.07454	0.38575	1.02868
116	O116	0.02613	0.41446	0.34347	159	S159	-0.01216	0.37657	0.61143
117	O117	0.10921	0.46779	0.38024	160	O160	-0.0537	0.35872	0.41127
118	O118	0.41808	0.38537	1.06641	161	O161	-0.02163	0.40186	0.87351
119	O119	0.40924	0.40502	1.00065	162	C162	-0.01371	0.3255	0.73655
120	Fe120	0.46928	0.42694	0.8397	163	F163	-0.01209	0.32348	1.06546
121	O121	0.53193	0.66373	1.30357	164	F164	-0.05109	0.28943	0.63239
122	O122	0.59269	0.66898	0.9225	165	F165	0.02003	0.32317	0.60751
123	Fe123	0.06133	0.47512	0.48688	166	O166	0.33694	0.98987	0.22243

167	O167	0.30153	0.89246	0.18212	195	O195	1.00578	0.64115	0.67102
168	Fe168	0.35907	0.94753	0.11453	196	C196	0.99094	0.69727	0.32847
169	S169	0.26765	0.8964	0.4442	197	F197	1.03262	0.72297	0.43084
170	O170	0.25137	0.91046	0.15036	198	F198	0.99006	0.70065	-0.00031
171	O171	0.24354	0.84583	0.42104	199	F199	0.96627	0.71309	0.46237
172	C172	0.32159	0.92192	0.59669	200	O200	0.61266	0.10561	0.60426
173	F173	0.3627	0.95648	0.56962	201	O201	0.56779	0.01729	0.45881
174	F174	0.31024	0.94255	0.80134	202	Fe202	0.5612	0.06762	0.35338
175	F175	0.32753	0.88801	0.69024	203	S203	0.60128	0.00943	0.20122
176	S176	0.33922	1.02883	-0.05514	204	O204	0.61586	0.04518	-0.05883
177	O177	0.36088	1.07192	0.14488	205	O205	0.64322	0.02632	0.39546
178	O178	0.37452	1.03905	-0.30494	206	C206	0.58643	-0.04487	0.03475
179	C179	0.28833	1.02307	-0.19288	207	F207	0.5509	-0.05981	-0.16006
180	F180	0.28426	1.05785	-0.08079	208	F208	0.62002	-0.04181	-0.14487
181	F181	0.28627	1.02285	-0.52156	209	F209	0.57741	-0.07459	0.28269
182	F182	0.25479	0.98416	-0.08043	210	S210	0.6586	0.14105	0.38578
183	O183	0.96317	0.59887	0.16823	211	O211	0.67268	0.11226	0.20316
184	O184	0.87856	0.55335	0.04722	212	O212	0.64225	0.15686	0.10474
185	Fe185	0.9181	0.53995	0.27002	213	C213	0.70651	0.18827	0.55657
186	S186	0.84643	0.56598	0.28732	214	F214	0.72649	0.17321	0.76184
187	O187	0.80429	0.54603	0.09363	215	F215	0.73445	0.21183	0.31054
188	O188	0.8303	0.53277	0.56305	216	F216	0.69623	0.2159	0.7203
189	C189	0.85688	0.62129	0.3888	217	H217	0.26665	0.71359	0.60758
190	F190	0.89475	0.65236	0.25285	218	H218	0.29753	0.61488	0.82754
191	F191	0.82427	0.62731	0.27431	219	H219	0.39766	0.74637	0.64071
192	F192	0.85902	0.62691	0.71631	220	H220	0.68948	0.31043	0.33123
193	S193	0.971	0.63968	0.44537	221	H221	0.68539	0.42892	0.45914
194	O194	0.93244	0.62063	0.67689	222	H222	0.56933	0.30505	0.42499

Table S16. Simulated topological models for Fe-COF_{TAPB-PDA} with corresponding cell parameters and porous properties.

Topological Models	Fe-COF _{TAPB-PDA}	COF _{TAPB-PDA} P6/m_AA	COF _{TAPB-PDA} P63/m_AB
Cell parameters $(\alpha = \beta = 90^\circ, \gamma = 120^\circ)$	$a = 36.2722 \text{ \AA}$ $b = 35.7041 \text{ \AA}$ $c = 5.1475 \text{ \AA}$	$a = b = 37.8094 \text{ \AA}$ $c = 3.4733 \text{ \AA}$	$a = b = 37.8241 \text{ \AA}$ $c = 6.3206 \text{ \AA}$
Free volume per cell (\AA^3)	1355.69	2399.52	2446.81
Surface area per cell (\AA^2)	689.69	386.20	1369.36
Surface area (m^2/g)	1328.25	2339.92	4110.31
Pore volume (cm^3/g)	0.261	1.454	0.734
Pore size (nm)	2.16	3.21	-

References

- S1 Riddell, I. A.; Ronson, T. K.; Clegg, J. K.; Wood, C. S.; Bilbeisi, R. A.; Nitschke, J. R., Cation- and Anion-Exchanges Induce Multiple Distinct Rearrangements within Metallosupramolecular Architectures. *J. Am. Chem. Soc.* **2014**, *136*, 9491-9498.
- S2 Hogue, R. W.; Dhers, S.; Hellyer, R. M.; Luo, J.; Hanan, G. S.; Larsen, D. S.; Garden, A. L.; Brooker, S., Self-Assembly of Cyclohelicate [M3L3] Triangles Over [M4L4] Squares, Despite Near-Linear Bis-terdentate L and Octahedral M. *Chem. Eur. J.* **2017**, *23*, 14193-14199.
- S3 L. N. Mulayand E. A. Boudreux, Theory and Applications of Molecular Diamagnetism, John Wiley& Sons Inc., New York, 1976.
- S4 Riddell, I. A.; Hristova, Y. R.; Clegg, J. K.; Wood, C. S.; Breiner, B.; Nitschke, J. R., Five discrete multinuclear metal-organic assemblies from one ligand: deciphering the effects of different templates. *J. Am. Chem. Soc.* **2013**, *135*, 2723-2733.
- S5 Brummel, O.; Faisal, F.; Bauer, T.; Pohako-Esko, K.; Wasserscheid, P.; Libuda, J., Ionic liquid-modified electrocatalysts: the interaction of $[C_1C_2Im][OTf]$ with Pt(111) and its influence on methanol oxidation studied by electrochemical IR spectroscopy. *Electrochim. Acta* **2016**, *188*, 825-836.
- S6 Bauer, T., Agel, F., Blaumeiser, D., Maisel, S., Görling, A., Wasserscheid, P., Libuda, J., Low-temperature synthesis of oxides in ionic liquids: ozone-mediated formation of Co_3O_4 nanoparticles monitored by in situ infrared spectroscopy. *Adv.*

Mater. Interfaces **2019**, *6*, 1900890.

S7. Gejji, S. P.; Hermansson, K.; Lindgren J., Ab initio vibrational frequencies of the triflate ion, $(\text{CF}_3\text{SO}_3)^-$. *J. Phys. Chem.* **1993**, *97*, 3712-3715.